



# Office of Graduate Studies

## Dissertation / Thesis Approval Form

This form is for use by all doctoral and master's students with a dissertation/thesis requirement. Please print clearly as the library will bind a copy of this form with each copy of the dissertation/thesis. All doctoral dissertations must conform to university format requirements, which is the responsibility of the student and supervising professor. Students should obtain a copy of the Thesis Manual located on the library website.

**Dissertation/Thesis Title:** Neural mechanisms of spatial navigation and memory

**Author:** Jonathan F. Miller

**This dissertation/thesis is hereby accepted and approved.**

**Signatures:**

Examining Committee

Chair \_\_\_\_\_

Members \_\_\_\_\_  
\_\_\_\_\_  
\_\_\_\_\_

Academic Advisor \_\_\_\_\_

Department Head \_\_\_\_\_

**Neural mechanisms of spatial navigation and memory**

A Thesis

Submitted to the Faculty

of

Drexel University

by

Jonathan F. Miller

in partial fulfillment of the

requirements for the degree

of

Doctor of Philosophy

June 2015



© Copyright 2015  
Jonathan F. Miller. All Rights Reserved.

## Dedications

To Nicole.

## Acknowledgments

First and foremost, I'd like to thank and acknowledge my thesis advisor Joshua Jacobs. I've known Josh since I was an undergraduate and he was a graduate student at the University of Pennsylvania, over a decade ago. Through all of this time, even well before I knew I'd be his student, Josh has been a source of knowledge and guidance. Josh has taught me how to be a successful scientist, and, moreover, Josh has given me a set of skills that I am confident will serve me well in the future. I'm grateful to call Josh my friend, and I'm looking forward to our continued friendship over the years to come.

I am also indebted to Michael Kahana, who I've worked with for many years, and with whom I still collaborate. It was because of Mike that I first became interested in neuroscience, and it was through working in his lab as an undergraduate that I first began to understand the excitement that comes from trying to unravel the mysteries of the human brain. I would also like to thank many current and former members of the Kahana lab, in particular those who have helped me with the arduous task of data collection, including Emily Rosenberg, Erin Beck, Ryan Baily Williams, Patrick Crutchley, Ashwin Ramayya, John Burke, Deb Levy, and Anastasia Lyalenko. In addition, I'm grateful for my current lab members, notably Tom Coffey and Sang Ah Lee, for their invaluable support and insights over the course of my graduate career.

These acknowledgments would be incomplete without mentioning my clinical collaborators at Thomas Jefferson University Hospital, the Hospital of the University of Pennsylvania, UCLA Medical Center, and Freiburg University Hospital. It is through their efforts that I am afforded the rare opportunity to collect human neural recordings. I'd also like to thank the patients themselves from whom I've collected data, who selflessly volunteered to participate in our studies and who made this entire endeavor possible.

Lastly, I'd like to thank my wife Nicole Long, whose love and support has kept me focused, and my parents, for their unending encouragement.



## Table of Contents

LIST OF TABLES . . . . .	vii
LIST OF FIGURES . . . . .	viii
ABSTRACT . . . . .	ix
1. INTRODUCTION . . . . .	1
1.1 Human intracranial recordings . . . . .	2
1.2 The neural representation of space . . . . .	3
1.3 Episodic memory and spatiotemporal context . . . . .	5
1.4 Overview . . . . .	6
2. NEURAL ACTIVITY IN HUMAN HIPPOCAMPAL FORMATION REVEALS THE SPATIAL CONTEXT OF RETRIEVED MEMORIES . . . . .	8
2.1 Abstract . . . . .	8
2.2 Introduction, Results, and Discussion . . . . .	8
2.3 Supplemental Materials and Methods . . . . .	16
2.4 Supplemental Figures . . . . .	26
2.5 Supplemental Tables . . . . .	29
3. REPEATING SPATIAL ACTIVATIONS IN HUMAN ENTORHINAL CORTEX . . . . .	31
3.1 Summary . . . . .	31
3.2 Results . . . . .	32
3.3 Discussion . . . . .	37
3.4 Experimental Procedures . . . . .	39
3.5 Supplemental Data . . . . .	41
3.6 Supplemental Experimental Procedures . . . . .	45
4. HUMAN HIPPOCAMPAL THETA AND ITS RELATIONSHIP TO SPEED, MEMORY, AND VOLUNTARY MOVEMENT . . . . .	51
4.1 Abstract . . . . .	51

4.2	Introduction . . . . .	52
4.3	Methods . . . . .	54
4.4	Results . . . . .	58
4.5	Discussion . . . . .	64
5.	GENERAL DISCUSSION . . . . .	68
5.1	Summary . . . . .	68
5.2	Regional differences in medial temporal lobe spatial coding . . . . .	70
5.3	Beyond space in the hippocampus . . . . .	71
5.4	From rodents to humans . . . . .	72
5.5	Future directions and concluding remarks . . . . .	73
	BIBLIOGRAPHY . . . . .	76

## List of Tables

2.1	Summary of place-responsive cells . . . . .	29
2.2	Place-responsive cells characteristics . . . . .	30
3.1	Summary of path equivalent cells . . . . .	45

## List of Figures

2.1	<i>Delivery Person</i> task design . . . . .	10
2.2	Place-responsive cells . . . . .	13
2.3	Timecourse of neural similarity . . . . .	14
2.4	Place-responsive cell firing rate by condition . . . . .	15
2.5	Spatial context reinstatement analysis method . . . . .	26
2.6	Spatial context reinstatement via individual cell firing rate analysis method . . . . .	27
2.7	View-responsive cell analysis method . . . . .	28
3.1	Behavioral task and performance . . . . .	32
3.2	Path equivalent cell firing rate maps . . . . .	34
3.3	Examples of path equivalent cells . . . . .	35
3.4	Population measurements . . . . .	37
3.5	Average occupancy map . . . . .	41
3.6	Firing rate maps and associated spiking activity . . . . .	42
3.7	Additional examples of path equivalent (PE) cells . . . . .	43
3.8	Spike cluster characteristics . . . . .	44
4.1	Linear track behavioral task . . . . .	54
4.2	Low frequency increases during virtual movement . . . . .	59
4.3	Relationship of power and movement speed . . . . .	61
4.4	Relationship of power and memory accuracy . . . . .	62
4.5	Relationship of power and automatic/manual movement . . . . .	63
4.6	Power modulation following changes in speed . . . . .	64

## Abstract

Neural mechanisms of spatial navigation and memory

Jonathan F. Miller

Joshua Jacobs, Ph.D.

The ability to navigate our environment is a vital skill for numerous species, including humans. How does the brain encode external space to allow for accurate navigation? Moreover, as we move through the world, how do we keep track of where specific events occur? Based on decades of research in rodents, we know that the hippocampus contains *place cells* that code for particular locations in the environment, and based on decades of work in humans, we know that the hippocampus is crucial for episodic memory function. The goal of this dissertation is to study how the human brain simultaneously supports spatial navigation and memory function by analyzing intracranially recorded EEG from participants performing virtual spatial memory tasks. In my first study, I investigated whether the neural representation of space formed by the place cell population code in the medial temporal lobe (MTL) becomes integrated with a broader memory signal. I found that place cells in human MTL act as a mechanism for memories to become linked to the location where they occurred, suggesting that the neural system underlying spatial navigation and the neural system underlying memory function are not as distinct as once thought. In my next study, I investigated whether anatomical subregions of the human MTL, specifically the entorhinal cortex (EC) and the hippocampus, differ in the type of spatial information that they are selective to, which has been shown to be true in rodents. I discovered a new type of cell in the human EC called *path equivalent cells* that provides a metric of distance relative to an environment's geometry, unlike hippocampal place cells that only fire at specific locations. This finding helps to bring our understanding of how space is represented in the human brain closer to our understanding of space in the rodent brain, which has been studied for many more decades. In my final study, I investigated how oscillatory activity in the human hippocampus is modulated by movement through the environment. In rodents, the *theta* oscillation (4–8 Hz) is closely linked to voluntary movement through space and is an integral component for many rodent derived theories of MTL function. I found that functionally analogous signals in human hippocampus appeared at lower frequencies than in rodents, suggesting that these theories may require modification before they can be broadly applied to other species. Taken together, my work helps to reconcile how the MTL supports both spatial navigation and episodic memory function, as well as bridging the gap between the large literature describing the neural representation of space in the rodent brain and the comparatively less well understood

mechanisms in the human brain.



## Chapter 1: Introduction

As we move through our lives, we also move through the world. We go from room to room within our homes, we commute from our homes to our workplace, we travel throughout our neighborhoods and cities, and we take vacations to explore new countries. As we move, we learn our way around our environment. We create an internal map - an internal representation of external space - that allows us to get from place to place, and, in addition, provides us with the means to keep track of where the events that we experience in our lives occur. We have the ability to both navigate our world and to form rich detailed memories as we move through it. Somehow, our brains support these dual abilities, which are fundamental to our daily quality of life.

Decades of neuroscience research have attempted to uncover the neural mechanisms responsible for spatial navigation and memory function, yet these two fields have largely been studied independently from each other. The investigation into the neural basis of spatial navigation was propelled forward over 40 years ago by the discovery of *place cells* in ambulating rats [O'Keefe and Dostrovsky, 1971]. Place cells are neurons, primarily located in the hippocampus, that fire action potentials whenever the animal is physically located at a particular spot in world. They are remarkable in that they reveal a clear mapping of external space onto a neural substrate, and they provided the first indication as to how the brain might create an internal, or cognitive, map of our surroundings. This finding, which has since earned discoverer John O'Keefe the 2014 Nobel prize in Physiology or Medicine, spawned an entire subfield of neuroscience focused on detailing the neural representation of space in the rodent hippocampus and the surrounding medial temporal lobe structures of the brain.

In contrast, our understanding of the neural underpinnings of memory function is rooted in human neurophysiology. When patient H.M. had his hippocampi removed to treat his medication-resistant epilepsy, he could no longer reliably form new memories [Scoville and Milner, 1957]. More specifically, he could no longer form new *episodic* memories, or memories for experienced events

[Tulving, 1972]. As with rodents and place cells, this discovery of a clear functional relationship between a neural structure – once again, the hippocampus – and an observable behavior served to focus much of the field’s future attention. In this case, it was focused on the role of the human hippocampus in supporting episodic memory function.

In spite of this historical delineation, the spaces we inhabit and the memories we form within those spaces are intricately linked. When we reimagine the past, be it what we had for breakfast today or a favorite childhood birthday party from decades prior, the location of the past event is one of the primary and salient features of the memory. A main goal of the work described in this dissertation is to bridge the divide between these areas of research, spatial navigation in rodents and memory for past events in humans, and simultaneously study spatial navigation and memory function using human neural recordings. In order to do so, I will first describe certain methodological details upon which my work is based, including how the neural data is collected and how human navigation and memory can be probed in an experimental setting.

## 1.1 Human intracranial recordings

Rodent place cells were discovered by recording *in vivo* activity from individual neurons using electrodes inserted into rodent hippocampus. To facilitate making comparisons to rodent research, the studies I perform here all make use of the rare opportunity to collect intracranial recordings of neural activity from electrodes implanted directly in the human brain. For clear ethical reasons, recording neural activity from the general population using direct brain implants is not justifiable. As a result, this work relies on data from the population of epilepsy patients who are undergoing monitoring for seizure localization. These patients all suffer from seizures that cannot be controlled through pharmacological intervention, thus they have elected to have electrodes placed subdurally (on the surface of the cortex) as well as to have electrode depth probes inserted into deeper brain structures, such as the hippocampus.

The goal of this procedure is to localize the area of the brain responsible for the generation of seizures, with the aim of ultimately resecting the seizure focus to reduce or eliminate seizure production. Patients remain in the hospital for ~1–3 weeks while their brain activity is being

recorded. The data collected using this method, known as either intracranial electroencephalographic (iEEG) or electrocorticographic (ECoG) recordings, provide the clinicians with a means of assessing which areas of the brain are epileptogenic, and the procedure results in significant reduction in seizure frequency in approximately 50% of patients [Kahana, 2006].

When patients are not occupied with clinical matters, they are often free to participate in cognitive studies, affording researchers a unique opportunity to measure the electrical activity of the brain recorded via direct contact with active tissue. The data collected with this methodology can be broken down into two distinct categories. First, one can analyze the signals recorded from macroelectrodes, which are relatively large contacts with diameters measured in the range of millimeters. These contacts record the activity of a  $\sim 4\text{mm}^2$  area of tissue, encompassing the summed activity of a large population of neurons. Signals recorded from these macroelectrodes are generally analyzed by either examining how the voltage potential changes as a function of experiment condition, or by decomposing the voltage time series into its constituent frequencies and determining how the power and phase of the signal at various frequencies is related to experimental conditions of interest.

The second type of data is collected from microelectrodes, which are much smaller than macroelectrodes, having diameters in the range of microns (in the case of the studies performed here, the microelectrodes have a diameter of  $40\mu\text{m}$ ). Microelectrodes extend from the tip of the depth probes inserted into deep brain structures, and, importantly, are small enough to measure the action potentials of individual neurons. Here, the unit of analysis is not necessarily the voltage or power signal, but is rather the timing and rate of neuronal spiking. This spiking data is analogous to the type of data that led to the discovery of place cells in rodents, allowing for similar analytic methods to be carried out with human data.

## 1.2 The neural representation of space

When place cells were discovered and their properties first studied in the 1970s, researchers had their first glimpse into the precise neural mechanisms supporting an organism's ability to self-localize within the external environment. Place cells, with their well-defined "place fields" that link a physical location to an internal representation [O'Keefe and Nadel, 1978], suggested a concrete mechanism

by which the brain stores a map of the world. With a large enough set of place cells, each one coding for a particular region of space, an animal's location at any given moment can be represented by the activity of the population of cells. Indeed, if enough simultaneous place cells are recorded, a rodent's position can be accurately reconstructed from the neural activity [Wilson and McNaughton, 1993, Zhang et al., 1998]. For a time, it seemed as though a pure cognitive map, as hypothesized by Edward Tolman decades prior [Tolman, 1948], had been found.

Over time, however, it has become clear the spatial representation system in the brain is much more complex. Not only are there place cells in the hippocampus that code for particular locations, but there are numerous other types of cells throughout the medial temporal lobe (MTL) that are tuned to specific environmental properties. For example, head direction cells in pre- and parasubiculum code for the direction the animal is facing [Taube et al., 1990], border or boundary cells in the entorhinal cortex (EC) code for locations near the edge of an environment [Solstad et al., 2008], and grid cells in the EC have non-localized firing fields that tessellate across an entire region of space [Hafting et al., 2005].

In addition to these specialized cell types, brain oscillations – the result of the summed activity of populations of neurons [Lachaux et al., 2003] – are closely tied to rodent spatial navigation. Of particular interest is the hippocampal *theta* oscillation, typically defined as 4–10 Hz, whose amplitude increases during periods of voluntary movement [Vanderwolf, 1969]. Moreover, theta is mechanistically related to the activity of spatially tuned cells. The theta oscillation is thought to play a key role in coordinating the timing of action potentials of place cells, such that the likelihood of firing varies as function of the phase of theta [O'Keefe and Recce, 1993, Skaggs et al., 1996]. Oscillatory interference models of EC grid cell generation causally rely on theta when explaining how grid cells are formed [Burgess et al., 2007]. The diversity of spatially tuned cells and their modulation by oscillatory activity raises questions about how all of this information is integrated and what roles different MTL structures may play in supporting navigation abilities.

In contrast to the large volume of work describing the neural representation of space in the rodent brain, there has been relatively little work investigating the same questions in humans. Place

cells and grid cells have indeed been shown to exist in human MTL [Ekstrom et al., 2003, Jacobs et al., 2010a, 2013], and low frequency oscillations are more prominent during periods of movement [Caplan et al., 2003, Kahana et al., 1999]. However, our knowledge of how the human brain represents external space still pales in comparison to our knowledge of rodents. Do the properties of spatially tuned cells vary based on brain region? Does the theta oscillation, with its strong functional ties to navigation in the rodent, act in an analogous manner in humans? Furthermore, with so much of the MTL seemingly dedicated to spatial processing, reconciling how the same part of the brain is vital for memory function in humans has been a challenge. An aim of my work is to investigate these issues with the same level of detail as they have been investigated in rodents.

### 1.3 Episodic memory and spatiotemporal context

Space is an intuitively vital aspect of our episodic memories. The events that we experience in our lives necessarily occur at a particular time, with particular surroundings, and at a particular location. This can be framed more formally by saying that events take place within a *spatiotemporal* context, such that we can remember both where and when an event occurred [Eichenbaum, 2004, Tulving, 1983]. Yet, throughout the history of episodic memory experiments, the study of the role played by spatial information has largely been ignored. In general, episodic memory experiments present study participants with lists of words or pictures to encode so that they can later be recalled or recognized, devoid of any spatial information. Thus, a major drawback of these traditional methods is that they lack a sense of real world ecological validity, as it has been shown that spatial information is a key element in memory formation, organization, and retrieval [Miller et al., 2013]. To overcome this limitation of previous studies, all of the work I will present makes use of virtual environments to extend experiments into three dimensions, allowing for the study of the neural representation of space, memory, and their interactions.

**Virtual navigation** To study the neural representation of space in the rodent, researchers generally record from a freely moving animal that is tethered to a recording system. Unfortunately for human research, the ability to record from the human brain comes with the cost of limited mobility.

When hospital patients perform iEEG experiments, they are either resting in their bed or sitting in their chair. To overcome this restriction, we create visually rich 3D environments that participants navigate on a laptop computer. While virtual tasks lack the locomotive and proprioceptive feedback of real navigation, previous studies of both rodent [Chen et al., 2013, Harvey et al., 2009] and human [Ekstrom et al., 2003, Jacobs et al., 2010a, 2013] spatial navigation have revealed that virtual navigation is sufficient to elicit neural responses similar to actual navigation in rodents. In addition, though we lose certain attributes of real world navigation, we gain the capability to precisely design and control the virtual environments to our exact specifications.

The virtual environments that I will describe were created using the Panda Experiment Programming Library (PandaEPL), which is an open source 3D experiment platform [Solway et al., 2013]. PandaEPL allows for the construction of freely navigable 3D environments, and importantly, incorporates extremely precise logging to accurately align patient activity in the task with the neural data.

## 1.4 Overview

We are all defined by our memories and past experiences, of which space is a core component. This is perhaps most evident when considering the profound effects of neurodegenerative diseases such as Alzheimer's, where the loss of memory function, along with spatial disorientation, are primary symptoms. As we move through space and time, we are constantly encoding new memories for later retrieval, transforming the events of our lives into patterns of brain activity. Understanding the neural underpinnings of this process is a lofty yet fundamental goal of neuroscience. Whether or not any animals possess episodic memory in a manner that is on par with humans is an open debate [Clayton et al., 2003], yet it is hard to dispute the claim that this goal, due to our combination of memory, language, and communication abilities, can only truly be accomplished through the study of the human brain.

The body of work that I will present is focused on two overarching themes. First, my work serves to extend our knowledge of how the brain represents spatial information by studying spatial navigation in humans. Directly comparing rodent findings with data from human studies is necessary

in order to validate theories of brain function that are derived mainly from the rodent literature. Second, I make use of the fact that memory in humans can be probed more explicitly than memory in animals to investigate how the brain represents the spatial components of memories, as well as to better understand what role these components may play in the general episodic memory engine.

In **Chapter 2**, I build upon our knowledge of the existence of place cells in humans to examine if place cells are simply an internal biomarker of location or whether they become integrated into a broader memory trace. To do so, I recorded the activity of individual medial temporal lobe neurons in patients performing a hybrid memory and spatial navigation task, and I found that place cells that were active during spatial navigation reactivated outside of navigation when patients recalled specific memory episodes. In **Chapter 3**, I add to our understanding of how the brain represents space through the discovery of new type of spatially tuned cell not previously seen in humans. I show that *path equivalent cells* encode distance traveled relative to environmental geometry, and, in line with rodent findings [Frank et al., 2000], that these cells tend to be localized to the entorhinal cortex. In **Chapter 4**, I use analyses of oscillatory activity to investigate whether the key role played by theta oscillations in rodent navigation and memory is conserved across species. While I found that many core attributes translated from rodents to humans, there do exist fundamental inter-species differences in the behavior of movement related oscillatory activity, highlighting the need to validate existing theories using human data. In **Chapter 5**, I synthesize these findings and relate them to the broader literature of both spatial navigation and memory function.

## Chapter 2: Neural Activity in Human Hippocampal Formation Reveals the Spatial Context of Retrieved Memories

Jonathan F. Miller, Markus Neufang, Alec Solway, Armin Brandt, Michael Trippel, Irina Mader, Stefan Hefft, Max Merkow, Sean M. Polyn, Joshua Jacobs, Michael J. Kahan, & Andreas Schulze-Bonhage  
*Science*, 342(6162): 1111–1114, 2013.

### **2.1 Abstract**

In many species, spatial navigation is supported by a network of “place cells” that exhibit increased firing whenever an animal is in a certain region of an environment. Does this neural representation of location form part of the spatiotemporal context into which episodic memories are encoded? We recorded medial temporal lobe neuronal activity as neurosurgical patients performed a hybrid spatial and episodic memory task. We identified place-responsive cells active during virtual navigation and then asked whether the same cells activated during the subsequent recall of navigation-related memories without actual navigation. Place-responsive cell activity was reinstated during episodic memory retrieval. Neuronal firing during the retrieval of each memory was similar to the activity that represented the locations in the environment where the memory was initially encoded.

### **2.2 Introduction, Results, and Discussion**

When one encounters an old friend and remembers the time they last met, often the place of meeting and surrounding circumstances come to mind. This is the hallmark of episodic memory—the capacity to store and later retrieve memories that are bound to a particular place and time [Tulving, 1983]. Theories of episodic memory posit that the brain supports this ability by continually maintaining an updated representation of the current spatiotemporal context, which is a neural representation of space, time, and other aspects of one’s current cognitive milieu [Polyn and Kahana, 2008]. When the brain forms a new episodic memory, these theories predict that the content of the experience becomes associated with the current spatial and temporal context. When the memory is retrieved, this prior context is partially reinstated, focusing one’s thoughts on time and place of the remembered episode.

This reinstatement not only provides the phenomenological experience of remembering, but it also helps to cue other memories experienced within the same or related contexts.

Although it is well established that the hippocampus and surrounding medial-temporal-lobe (MTL) structures play a central role in the formation and retrieval of context-mediated memories [Davachi, 2006, Eichenbaum, 2004, Scoville and Milner, 1957], we know far less about how these memory processes manifest in the activities of individual MTL neurons. Much of what is known about the neural coding properties of hippocampal and MTL neurons comes from studies of rodent spatial navigation, where individual neurons respond preferentially at specific locations within a given contextually-defined spatial environment [McNaughton et al., 2006a, O’Keefe and Nadel, 1978]. Similar neuronal responses have also been identified in the human hippocampus during virtual spatial navigation [Ekstrom et al., 2003, Jacobs et al., 2010a]. The context dependent firing of these neurons [Leutgeb et al., 2005a, Muller and Kubie, 1987] and their dependence on the animal’s goal state or past history of experienced cues [Ferbinteanu and Shapiro, 2003, Wood et al., 2000] has led some to speculate that the neural representation of space in the hippocampus is part of a broader network of neurons that encode episodic memories more generally [Buzsáki, 2005, Buzsáki and Moser, 2013, Eichenbaum et al., 1999, Howard et al., 2005]. This hypothesis suggests that the same neural structures and computations that enable the learning of a spatial layout via place cell activity also facilitate encoding episodic memories. However, according to a prominent alternative account, the spatial coding functions of the hippocampus are part of a context module that operates independently of the computations that encode the content of a memory [Davachi et al., 2003, Hargreaves et al., 2005].

We designed a virtual-reality memory game in which subjects played the role of a delivery person, driving through a virtual town and delivering objects to stores. Our subjects were patients with drug resistant epilepsy who were implanted with depth electrodes to localize the focus of their seizures and to map cognitive function in surrounding healthy tissue. In an initial phase of the game, subjects explored the town using a computer controller to navigate from store to store as they attempted to learn the layout of the environment illustrated in Fig. 2.1A. After this initial familiarization phase,

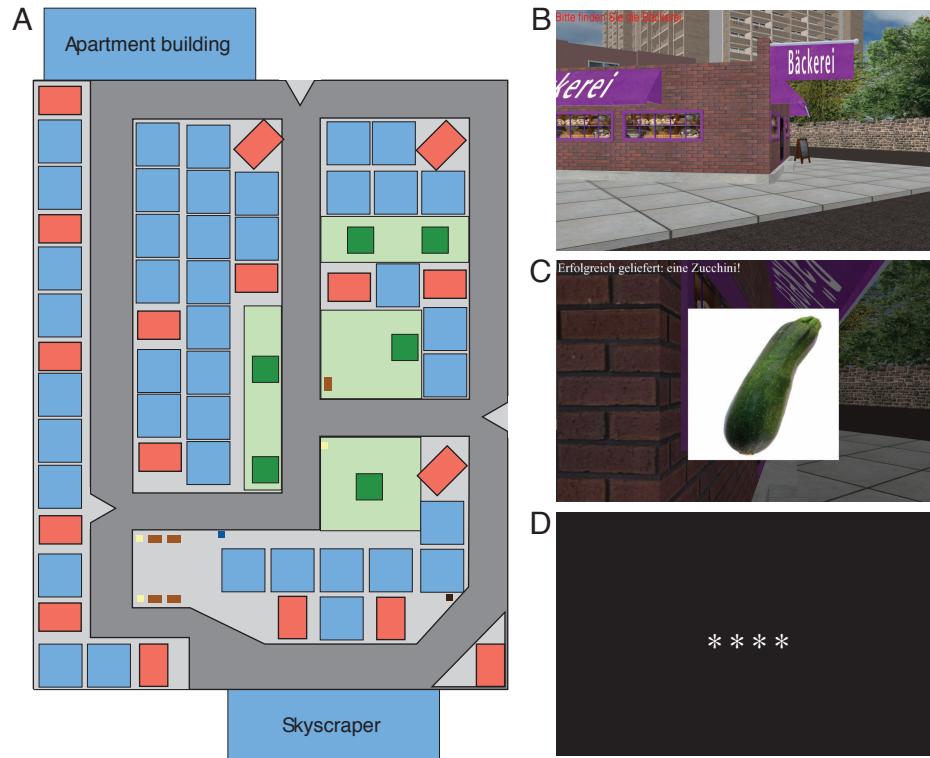


**Figure 2.1:** The behavioral task. **A.** Overhead map of the virtual environment. Red rectangles indicate store locations, and blue squares indicate locations of non-store buildings. Green areas indicate grass and trees, and the small dark blue, brown, and yellow boxes represent mailboxes, benches, and street lights. **B.** An example storefront that a subject might encounter. **C.** The presentation of an item (a zucchini) upon arrival at the target store (bakery). **D.** The initiation of the recall period, as indicated by a black screen with asterisks.

during which subjects visited each store twice, they began a series of “delivery days”. On each delivery day, subjects were instructed to travel from store to store, visiting 13 randomly chosen stores (of the 16 total) in a randomly determined order. Upon their arrival at each store, they were presented with an object (either visually for 2 sec for subjects 1 - 5 or aurally for subjects 6 - 7). Upon arrival at the final (13th) store, no item was presented. Instead, the screen went black and subjects were prompted to vocally recall as many of the 12 delivered objects as they could remember in any order (subjects recalled 5.2 objects, on average). After being given 90 seconds for free recall, subjects could advance to a new delivery day, in which they would deliver a unique but randomly determined set of objects to a random sequence of 13 stores and then attempt to recall the new set of objects. Consistent with prior work [Miller et al., 2013], subjects exhibited a significant ( $p = .008$ ) tendency to consecutively recall objects delivered to more spatially proximate locations (see supplementary text).

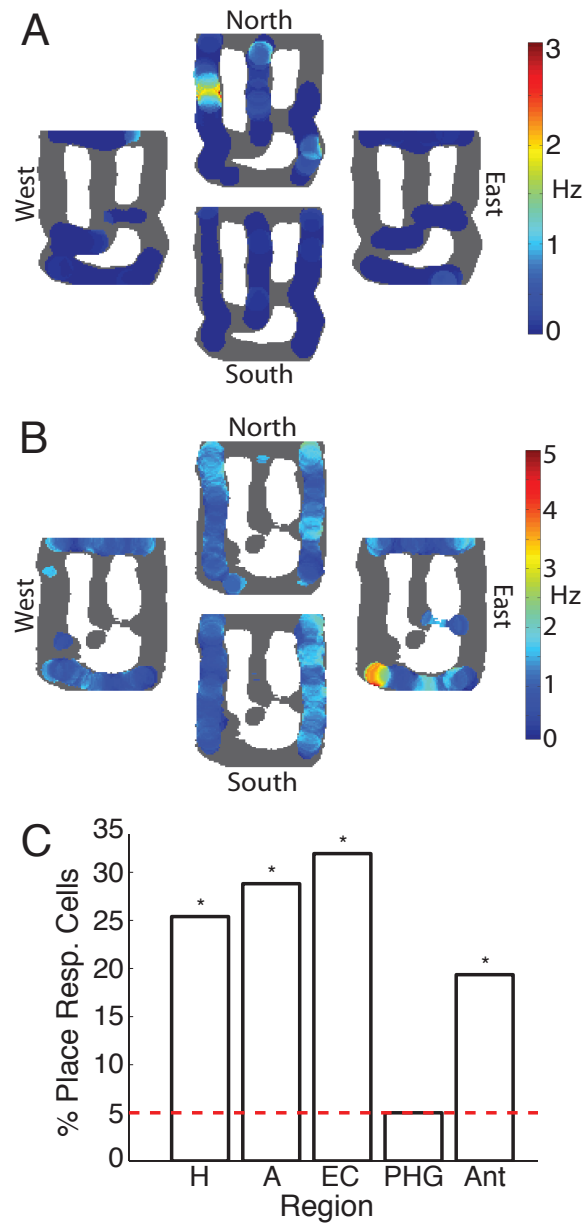
We first sought to identify patterns of neuronal activity that represented subjects’ location within the virtual town. We identified place-responsive cells as the neurons that exhibited significantly increased firing at a particular location in the virtual environment. Fig. 2.2A depicts the activity of one example place-responsive cell, which increased its firing rate when the subject was positioned at a location on the left side of the virtual environment and facing north. The majority of the identified place-responsive cells were direction dependent (72%) and did not exhibit significant place fields when direction of traversal was not taken into account. This is similar to prior findings of directionally oriented place cells in environments with clearly defined routes, in contrast to open environments, where omnidirectional place cells are prevalent [Ekstrom et al., 2003, Muller et al., 1994]. These directionally-oriented place cells were not generally responsive to place-invariant view information. Fig. 2.2B shows the firing rate of a place-responsive cell from the entorhinal cortex, which activated at a location in the south part of the environment during eastward movements. In total, we identified 95 place-responsive cells, comprising 25.6% of all observed neurons. There were significant numbers of place-responsive cells in the hippocampus, entorhinal cortex, amygdala, and in anterior MTL regions of ambiguous localization (binomial test with  $p < 0.01$  for each region,

Fig. 2.2C, Tables 2.1 and 2.2).

To determine whether spontaneous retrieval of items during free recall reinstated the spatial context associated with the item's encoding, we calculated the neural similarity between ensemble place-responsive cell activity during navigation and during item retrieval (see Fig. 2.5 for further details). We partitioned the environment into three regions for each recalled item: regions close to the delivery location, regions of intermediate distance, and regions that were far from the delivery location. We then asked whether the ensemble place-cell activity at the time of retrieval was more similar to navigational epochs that were closer to the delivery location. A high degree of similarity would indicate the reinstatement of the spatial context associated with the item. To protect against potential confounding between object and spatial context, we excluded navigational epochs surrounding the delivery of an object.

We found significant spatial context reinstatement surrounding the time of item vocalization (timecourse illustrated in Fig. 2.3A). The level of neural similarity between recall activity and navigation activity was ordered such that areas of the environment near an item's encoding location exhibited the highest similarity scores, intermediate spatial distances exhibited middling similarity scores, and far spatial distances exhibited the lowest similarity scores (this effect being strongest in the -300 to 700 ms interval illustrated in Fig. 2.3B). An ANOVA indicated a significant effect of distance bin on the level of neural similarity ( $F(2,300) = 7.6, p < .001$ ). Performing this latter analysis across subjects rather than recall events revealed that neural similarity within the near distance bin was significantly greater than neural similarity within the far distance bin (Fig. 2.3C,  $t(5) = 4.0, p = .009$ ).

During the spontaneous recall of an item, place-responsive cells exhibited firing patterns similar to those they showed during exploration of the region of the town where the item was previously delivered. Thus, recalling an episodic memory involves recovery of its spatial context, as seen in the activity of place-responsive cells in the human hippocampal formation and surrounding MTL regions. If the object delivery occurred in or near a cell's place field, characterized by a significantly higher than baseline firing rate, then recalling the object should also produce an increase in firing



**Figure 2.2:** Place-responsive cells. **A.** Firing rate map for a cell responsive to northward traversals located in Subject 6's hippocampus, shown separately for each cardinal direction. Grey represents all areas traversed by the subject, regardless of direction of travel. **B.** A cell responsive to eastward traversals recorded from Subject 1's entorhinal cortex. **C.** The regional distribution of place-responsive cells in the entire dataset of 371 single units (H: hippocampus, A: amygdala, EC: entorhinal cortex, PHG: parahippocampal gyrus, Ant: anterior MTL, not otherwise specified). The red line indicates the false positive rate of 5%.

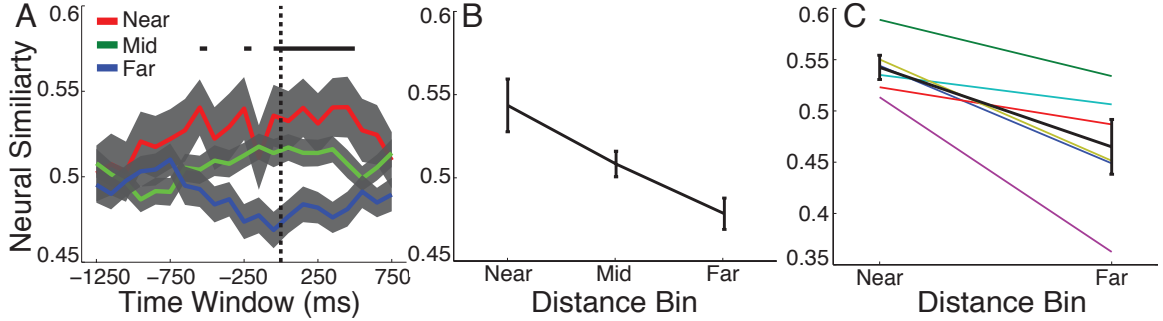


**Figure 2.3:** **A.** Timecourses of neural similarity between ensemble place cell activity during navigation and during item recall are shown for near, middle, and far spatial distance bins. Timecourses, shown relative to recall onset, were computed in overlapping 500-ms windows (x-values indicate the center of the window). Similarity is defined as the cosine of the angle between ensemble activity during recall and navigation, normalized as a rank score. Shaded regions indicate standard error of the mean across recalled items. The horizontal bar indicates significant timepoints as determined by an ANOVA with a false discovery rate adjusted significance threshold of 0.017. **B.** The average neural similarity for near, middle, and far spatial distance bins are shown for the time period -300–700 ms relative to recall onset. Error bars indicate standard error of the mean across recalled items. **C.** The neural similarity for near and far spatial distance bins for each of the included subjects (thin colored lines) and the subject average (thick black line) are shown for the time period -300–700 ms relative to recall onset. Error bars indicate standard error of the mean across subjects.

rate. We calculated the firing rate of place-responsive cells when subjects were navigating inside and outside of each cell's place field, as well as the firing rate when subjects recalled items that were presented near to or far from each cell's respective place field (Fig. 2.4) (see Fig. 2.6 for further details). The average in-field firing rate (3.8 Hz) was substantially higher than the out-of-field firing rate (1.9 Hz;  $t(32) = 5.9, p < 10^{-5}$ ). The average firing rate during the recall of items presented near a place field was 2.2 Hz, which was significantly higher than the 1.8 Hz firing rate during recall of items presented far from a place field ( $t(32) = 2.2, p = .03$ ).

Unlike traditional list recall studies of episodic memory, where items unfold only in time, the present experiment provided a unique spatial context for each item. This allowed us to leverage the spatial-coding properties of hippocampal neurons in the study of the neural basis of episodic recollection. Spatially-sensitive neural activity in the hippocampal formation became reactivated during episodic retrieval, when no visual cues were present. At the time of recall, subjects simply vocalized the names of the delivered objects in the order they came to mind, yet the neurons responsive to spatial information reactivated during the time just before and during vocalization.

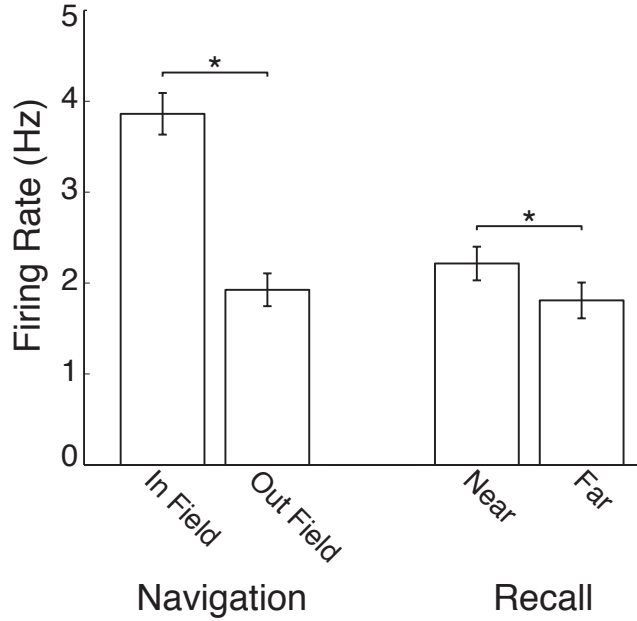


**Figure 2.4:** Place-responsive cell firing rate by condition. **Navigation.** In Field indicates the average place-responsive cell firing rate when navigating within a cell’s place field, whereas Out Field indicates the average place-responsive cell firing rate at locations outside of a place field ( $p < 10^{-5}$ ). **Recall.** Near indicates the average place-responsive cell firing rate in time period -1.5 s before to 1 s after recall onset of items that were initially presented in or close to the center of a place field, and, in contrast, Far represents the average place-responsive cell firing rate in the same time window for recall of items that were initially presented far from the center of a place field ( $p = .03$ ).

This reactivation implies that each experienced item is bound to its spatial context, which in turn may be reinstated when the item comes to mind during recall.

Because human neural recordings are rarely possible, little is known about the neural substrates of spontaneous verbal recall. Nonetheless, several recent studies have established the general phenomena of content reinstatement, whereby the attributes of an item at encoding become reinstated just prior to recall. This has been shown for human hippocampal neurons that are selective for taxonomic categories, or possibly individual items [Gelbard-Sagiv et al., 2008], and also for distributed patterns of intracranial EEG and hemodynamic activity [Manning et al., 2012, Polyn et al., 2005]. Reinstatement is not specific to an individual item but also spills over onto neighboring items as would be expected if those neighboring items provide an abstract temporal context for the recalled item [Howard et al., 2012, Manning et al., 2011]. Such a temporal context signal may be reflected

in the recent discovery of individual neurons in the rodent hippocampus that appear to encode the relative times of behaviorally significant events [MacDonald et al., 2011, Pastalkova et al., 2008].

Our finding that spontaneous recall of an item reactivates its spatial context provides direct neural evidence for theories of episodic memory that postulate context reinstatement as the basis for recollection [Polyn and Kahana, 2008, Polyn et al., 2009a]. It also argues that the spatial coding identified with the hippocampal place cell system is part of a more general engine of episodic memory in which items become associated with their spatiotemporal contexts and retrieval of items reinstates those contexts to help cue other context-appropriate memories.

### **2.3 Supplemental Materials and Methods**

Seven patients volunteered to participate in this research protocol, which was approved by the institutional review boards at both the University Clinic in Freiburg, Germany, and the University of Pennsylvania. The patients participated in a total of 65 delivery days spread across 16 experimental sessions each lasting approximately 1 hr. Across these sessions, we successfully isolated a total of 371 putative neurons from microelectrode recordings in the MTL. Among these 371 units, 189 were from the hippocampus, 72 were from the entorhinal cortex, 59 were from the amygdala, 20 were from the parahippocampal gyrus, and 31 were localized to the anterior MTL, but not a specific subregion (Table 2.1). See “Data Acquisition” below for a further description of localization methods. A small number of units recorded outside of these MTL regions are excluded from subsequent analyses.

#### **“Delivery Person” Task**

Subjects performed a hybrid spatial navigation—episodic memory task in which they played the role of a delivery person, delivering objects to stores in a virtual town. The task consisted of an initial familiarization phase during which subjects learning the locations of all of the stores in the virtual town, followed by a series of “delivery days”. On each delivery day, subjects delivered a set of pseudorandomly chosen objects to a subset of the stores and then the screen went blank and they were instructed to recall as many of the delivered objects as they could remember in any order. In this sense, each delivery day was analogous to a study-test trial of a traditional free recall task.

The virtual town was made up of 16 unique stores (chosen randomly from a pool of 22 stores) and 42 buildings, along with trees, benches, mailboxes, street lights, and areas of grass. Though the subset of stores chosen at the start of a session differed, the layout of the town was constant. Each store was modeled with a distinct storefront and unique visual features, allowing them to be easily recognizable. Subjects navigated the environment using a game controller to modulate direction of movement with movement being restricted to roads. The 3d models used in the virtual environment were created using Autodesk Maya<sup>TM</sup>. The environment was displayed to subjects using the Panda Experiment Programming Library [Solway et al., 2013], which is an in-house Python based wrapper around Panda3d, an open source game engine.

During the familiarization phase at the start of a session, subjects were instructed to navigate to each of the 16 stores twice, in a randomly determined order. The current target store was indicated via a text overlay at the top right of the screen (i.e., “Bitte finden Sie die Bäckerei”, which translates as “Please find the bakery”). After completing the familiarization phase, subjects began a series of delivery days, during which a text overlay instructed the subject to locate a specific store. Upon arrival at the store, a common object was presented. For subjects 1-5, the image of an object, randomly drawn from a pool of 208 distinct object images, appeared for 2 seconds. Because this version of the task was fairly challenging for subjects, we modified the procedure to use objects that were thematically related to stores. For subjects 6-7, objects were chosen from a pool of 420 objects that were thematically related to the stores (approximately 20 possible objects could be delivered to a given store). The names of these objects were previously recorded by a female speaker with clear diction and presented auditorily by the computer during the game. This change from visual to auditory object presentation was made so that the subjects would hear the object name while viewing the store. Presented objects could not be repeated within an experimental session. Each delivery can be thought of as an item presentation in a list learning experiment. After the object presentation, the text overlay instructed subjects to locate a different store. Subjects traveled to 13 randomly selected stores in the town (target stores did not repeat within a single delivery day). Objects were presented at the first 12 stores, and upon arrival at the 13th store, the screen went

blank, a row of asterisks appeared on the screen, and a tone sounded, which signaled the start of the free recall period. Subjects were given 90 seconds to attempt to recall any of the just delivered items, in any order. Subjects completed between 1 and 10 delivery days in a single recording session, depending on subject time constraints and willingness.

## Data Acquisition

Recording electrodes were placed in target regions selected on purely clinical grounds. Three to six Behnke-Fried electrodes per patient were stereotactically inserted into medial temporal and neocortical structures. Each Behnke-Fried electrode contained 9 platinum-iridium microwires with a diameter of  $40\ \mu\text{m}$  extending a few millimeter into the tissue at the tip of the electrode. Eight microwires, insulated except for the tip, were used for recording, while the 9th microwire was uninsulated and used as a reference. Electrodes were localized post-operatively on 3D MP-RAGE MRI. Precise neuroanatomic regions were determined using post-implant MRIs. Three neuroradiologists independently evaluated the positions of the electrodes. An electrode was labeled as being in a given region (hippocampus, amygdala, entorhinal cortex, parahippocampal gyrus) if at least two of the three localizations were in agreement. Electrodes for which there was disagreement among the localizations were grouped according to their position in the antero-posterior axis and labeled as either anterior or posterior. To eliminate any possibility of bias, the doctors performed the localizations using only unlabeled brain images, and thus were unaware of the type of neuronal activity observed from each electrode.

Signals from the microwires were recorded with three to six 8-channel amplifiers at a 20kHz sampling rate with an AD-converter resolution of 16 bits. The signal was low-pass filtered at 5 kHz and high-pass filtered at 0.02 Hz using built-in hardware filters. NeuroExplorer software was used for data acquisition and storage. Continuous recordings were started on the day of surgery or the 1st postoperative day and lasted for 5-10 days with 2-4 interruptions for clinical procedures. Spike detection and sorting was performed using WavClus v. 2.0 [Quiroga et al., 2004], which first detects spikes and then clusters them based on their wavelet coefficients. To avoid contamination between channels, recording channels were excluded if they shared greater than 50% of their spikes with

another channel on the same depth probe. Single-units with mean firing rates less than 0.1 Hz or greater than 15 Hz (potential interneurons) were excluded from analyses.

## **Analysis methods**

Behavioral navigation data was discretized into 250 ms epochs, and the subject's average x- and y-coordinate, heading (binned into cardinal directions), and speed within each 250 ms bin was calculated. We excluded navigation epochs during which subjects were not moving from the analyses. Audio recordings of the free recall portions of the task were annotated to identify each spoken word and mark its time of onset and offset within the audio file. This was done using TotalRecall—an open source software project designed for annotating recall data [Solway et al., 2010].

### **Identifying place-responsive cells**

Place-responsive cells were identified by using a rank-sum test to locate areas of the virtual environment where the cell exhibited significantly elevated firing (following similar methods as described in [Jacobs et al., 2010a]). The virtual environment was divided into a  $100 \times 100$  grid (VR-units). At each location, a one-tailed Wilcoxon rank-sum test compared the firing rates for all navigation epochs within a 10 VR-unit radius (nearby) to the firing rates for all other navigation epochs (far). There must have been at least 20 nearby epochs for a grid location to be included.

To determine our significance threshold, this procedure was repeated 100 times with time-shifted firing rate values, whereby the firing rate of the cell in each 250 ms epoch was randomly shifted relative to the navigation data. For each time-shifted dataset, we calculated the p-value threshold at which we would observe at least one place field. A place field was defined as a contiguous area of the environment greater than 2% of the total traversable area where the p-values fell below the given threshold. We then took the fifth percentile of p-value thresholds for the time-shifted data as our significance value for the unshifted data. This procedure fixes the Type 1 error at 5%. To test for place-responsive cells that may exhibit direction specific firing, this whole procedure was repeated separately for each cardinal direction. Here, the nearby firing rate for each grid location only included navigation epochs when the subject was traveling in a given cardinal direction, while the far firing

rate included epochs irrespective of direction of travel. We labeled a cell a place-responsive cell if a place field was discovered in any of these conditions. Because most place-responsive cells exhibited a preferred direction, it is possible that some of these cells responded to particular spatial scenes present while traveling in that cardinal direction. To help rule out this possibility, we carried out a further analysis of view-responsive cells, as described below. In brief, we did not find significant counts of view-responsive cells in our dataset.

### **Spatial context reinstatement via ensemble activity**

We excluded sessions with fewer than four place-responsive cells, leaving 12 separate recording sessions from six subjects, with a total of 105 recalled words and 78 place-responsive cells. We tested for spatial-context reinstatement by comparing the similarity of population neuronal responses between memory retrieval and spatial navigation. First, we characterized the neural representation of location during navigation by calculating the mean firing rate of each place-responsive cell in each location within a  $5 \times 7$  grid spanning the environment. We then organized this information by computing a series of population “place vectors” (one for each grid location), each of which characterized the mean pattern of neuronal activity across the subject’s place-responsive cells. Place vectors were only computed for locations that were traversed at least 10 times. In calculating the activity of place-responsive cells, we also excluded epochs in which objects were delivered, as well as a 250 ms buffer surrounding the object deliveries. This was done to help protect against potential confounds between item and spatial-context reinstatement.

Next, we characterized the place-responsive cell activity during episodic memory retrieval. For each item recall, we created a population “recall vector”, comprised of the mean firing rate of each place-responsive cell in a time period surrounding item vocalization. In order to ensure that the recall vector corresponded to only one memory retrieval, we did not compute recall vectors for items that were not sufficiently isolated (defined as another vocalization occurring within the preceding 1500 ms or the following 1000 ms), or for the first recall in the retrieval period. Next, we measured the degree to which recalling an item involves the reinstatement of the neural pattern that represented the location in the environment where the item was encountered. To quantify this spatial-context

reinstatement, we calculated the cosine similarity between each recall vector and each of the place vectors. For each recall vector, we then ranked the grid locations based on the similarity of the recall vector with grid locations' associated place vectors (that is, the grid location whose place vector has the highest similarity to the recall vector received a rank of 1). The rank-order transformation of cosine similarities helps to reduce variability from overall shifts in ensemble navigation-retrieval similarity, which would add noise to our analyses.

The context-reinstatement hypothesis predicts that for a given recall vector, place vectors from locations near the position where the item was encountered would have a higher level of similarity compared to the similarity to place vectors representing locations far from the item's delivery location. We tested this by, for each recall vector, binning the place vectors into three groups based on euclidean distance to the item's delivery location (near: less than 2, middle: greater than or equal to 2 and less than 4, or far: greater than 4). We then computed the mean rank of the place vectors in each group. We tested for significant spatial-context reinstatement across all item recalls by using an ANOVA to test for a significant difference in similarity between place vectors from different distance bins. See Fig. 2.5 for a graphical representation of this analysis.

To determine the time period relative to recall onset that exhibited significant reinstatement of place-responsive cell activity, the calculation of recall vectors, similarity scores, and significance values was repeated for twenty-one 500 ms overlapping time windows, beginning 1500 ms prior to recall onset and incremented by 100 ms until 500 ms post item onset (results shown in Fig. 2.3A of the main text). The resulting p-values were corrected using a False Discovery Rate (FDR) set at 0.05 to control for multiple comparisons [Benjamini and Hochberg, 1995]. Based on the results of this analysis, one set of recall vectors, one set of similarity scores, and the significance value were recalculated within the largest consecutive block of significant time windows (time windows beginning -300 ms through to 200 ms, thus the 1000 ms period of -300 ms through 700 ms; results shown in Fig. 2.3B of the main text).

We also determined whether the spatial reinstatement effect was present when first computing mean similarity scores within each subject, using the same -300 ms to 700 ms time window as above

(results shown in Fig. 2.3C of the main text). Instead of averaging across all recalls, we averaged each subject's near and far similarity scores to obtain subject specific measures. Data from subjects with multiple sessions were first concatenated. A t-test compared the distribution of near similarity scores to far similarity scores.

### **Spatial context reinstatement via individual cell firing rate**

Using the same subset of sessions as in the previous ensemble reinstatement analyses, we performed a separate analysis comparing the firing rate of each place-responsive cell during the recall of items initially presented near a place field to the recall of items initially presented far from a place field. We first calculated the firing rate of each place-responsive cell when subjects were navigating inside and outside of a cell's place field. As above, place fields were defined as a contiguous area greater than 2% of the traversable environment for which the significance values fell below the computed threshold (based on the described permutation procedure). If a cell exhibited a place field in more than one cardinal direction, the mean of the in-field and out-field firing rates for all included directions was calculated.

Next, for each cell and for all included recalled items, we determined if each recalled item was initially presented close to or far from the cell's place field. Here, near is defined as having been presented within a radius equal to the length of the place field's major axis, extending from the field's center of mass, and far is defined as having been presented outside of a radius equal to twice the place field's major axis, extending from field's center of mass (see Fig. 2.6 for a graphical representation of the division of the virtual environment). Then, we calculated the average firing rate of the cell within a window beginning 1.5 seconds before and extending 1 second post recall onset. Only cells that contributed data to both conditions were included in the analysis, limiting the number from 78 to 33 cells (for instance, not every cell had a set of recalled items that included initial presentations both near to and far from the place field).

### **Identifying view-responsive cells**

In a previous study of place-responsive cells during human virtual navigation, [Ekstrom et al., 2003] identified view cells that were predominantly found in the parahippocampal region. Because place

and view information can be correlated, we carried out an analysis of view cells to determine whether our finding of spatial context reinstatement was likely to have been driven by view rather than place-cell activity. We first divided the environment into 22 discrete location and direction dependent regions defined by the presence and visibility of specific landmarks, following the analysis framework outlined in [Ekstrom et al., 2003]. As stores were the most salient objects in the environment, regions of the environment in which a specific store was clearly visible were treated as a single region, reducing the overall number of regions to 17. We also defined regions in which no specific store was visible but which contained consistent views (for example, of a tall apartment building; see Fig. 2.7 for a schematic of the binning of the environment). Only epochs of movement in which the direction of travel (heading) was within 15 degrees of parallel to the corresponding region were included (this was to ensure consistency of view information). Then, for each cell, we performed a one-way ANOVA of the firing rate with region as the grouping variable (regions with less than 20 observations were excluded). We next repeated the analysis 100 times with time-shifted firing rate values, in which the firing rate of the cell in each 250 ms epoch was randomly shifted relative to the navigation data. To be labeled a view-responsive cell, we required that the true ANOVA p-value (calculated on the unshifted data) was less than the 5% percentile in the distribution of p-values found using the time-shifted data. Results of this analysis are reported in the supplemental text, below. To determine if these view-responsive cells could be responsible for the reinstatement effects, we reran the reinstatement analyses, excluding any place-responsive cells that were also labeled as view-responsive. For the spatial context reinstatement via ensemble activity analysis, we used the previously identified -300 ms through 700 ms time interval. Results of this analysis are reported in the supplemental text, below.

### **Spatial clustering of recalls analysis**

We calculated a spatial clustering score to determine whether our subjects, on aggregate, exhibited knowledge of the locations of the delivered objects. The spatial clustering score is a measure of the tendency for items delivered to spatially proximate locations to be recalled consecutively during the retrieval period [Miller et al., 2013]. To calculate this score, for each trial, every transition between a

recalled item and the following item is ranked based on the distance between their delivery locations. If the Euclidean distance between the delivery locations of two consecutively recalled items is the shortest of all the possible distances, that transition will be given a score of 1 (conversely, if it is the longest, it will be given a score of 0). For each trial, we calculated an average score, and then we averaged across all 65 trials in our dataset. To calculate the significance level of this score, we repeated this procedure 1000 times, each time randomly permuting the order of the recalled items (while maintaining the same recalled items). This randomization procedure disrupts any spatial clustering that may be present in the recall sequence beyond what would be expected by chance given the subset of recalled items. We then calculated a p-value by seeing where in this distribution the true spatial clustering score lies.

### **View-responsive cells**

We identified 18 view-responsive cells, which was below the Type-I error rate of 19. This failure to detect significant numbers of view-responsive cells is perhaps not surprising in light of the fact that we recorded comparatively few neurons in the parahippocampal region. Of the 18 view-responsive cells, 8 also met our criteria for place-responsivity. Although the number of view-responsive cells was not reliably greater than expected by chance, we nonetheless confirmed that our spatial context reinstatement effect was robust to the exclusion of these 8 cells. Recalculating the effect for the same interval as reported in our main analysis (-300 to 700 ms) revealed a significant difference between the spatial distance bins both on the level of recalls ( $F(2,297) = 5.6, p < .01$ ) and on the individual participant level ( $t(5) = 3.9, p = .01$ ). Additionally, we recalculated the distributions of place-responsive cell firing rates during the recall of items initially presented near and far from place fields, excluding any view-responsive cells from the analysis (lowering the number of included cells from 33 to 31). The average firing rate during the recall of items presented near a place field was 2.3 Hz, significantly higher than the 1.9 Hz firing rate during recall of items presented far from a place field ( $t(30) = 2.3, p = .03$ )

### Spatial clustering

The spatial clustering score for our dataset was .54, significantly greater than the chance level determined by the permutation procedure ( $p = .008$ ). Though our data were too sparse to determine significance of spatial clustering within individual subjects, we note that 6 out of 7 subjects exhibited greater than chance spatial clustering scores.

## 2.4 Supplemental Figures

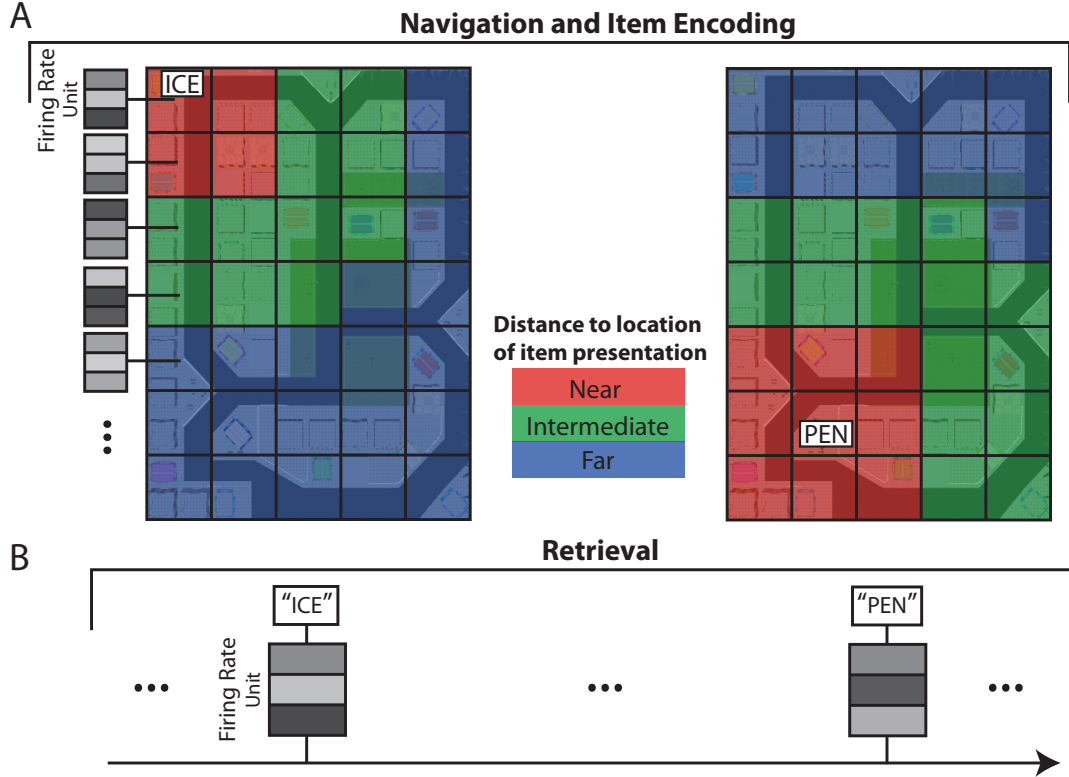


**Figure 2.5:** A schematic of the spatial context reinstatement via ensemble activity analysis. In these hypothetical examples, an item is presented to the subject in a particular sector of the town, as indicated in Panel A. Red shading indicates sectors considered spatially close the presentation location, green shading indicates sectors considered spatially intermediate, and blue shading indicates sectors considered spatially far. In a given session, the mean firing rate of all identified place-responsive cells was calculated separately for each sector (represented visually by the shaded grey boxes). During retrieval of the same item, the mean activity of the place-responsive cells was calculated. **A.** Two examples of the spatial binning of the environment. Left: the spatial binning of the environment if an item (“Ice”) was presented in the location indicated. Right: the spatial binning of the environment if an item (“Pen”) was presented in the location indicated. **B.** In the retrieval period, the mean place-responsive cell firing rate during each item recall is calculated and compared the navigation activity (recall of “Ice” uses the spatial binning shown in panel A Left and recall of “Pen” uses the spatial binning shown in panel A Right).

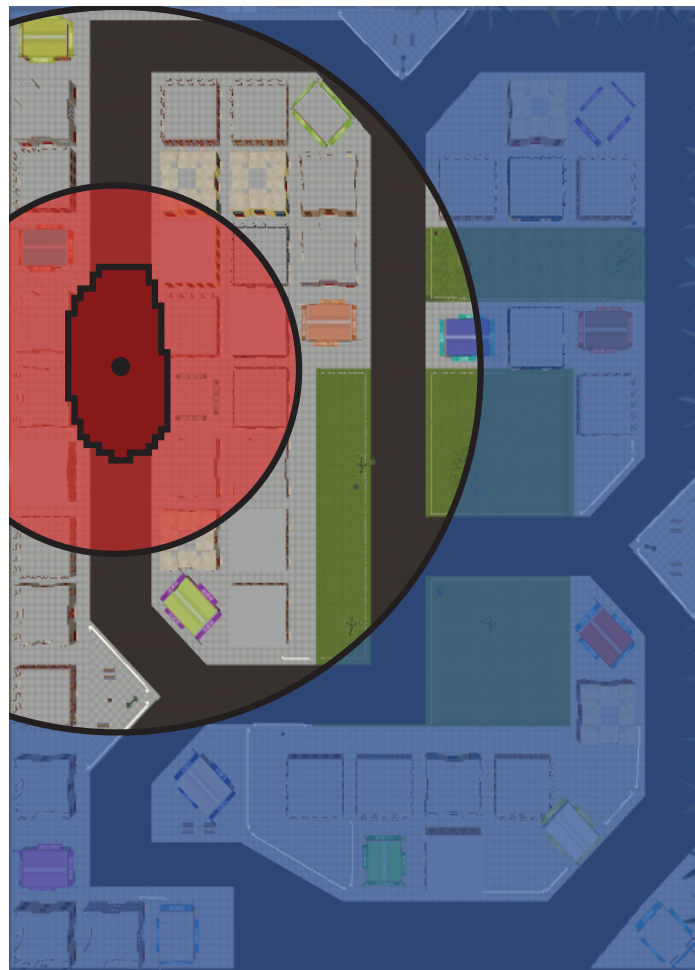


**Figure 2.6:** A visual representation of the spatial context reinstatement via individual cell firing rate analysis. The dark red area represents a cell's place field, and the dot in the middle of the place field represents the center of mass. Items delivered to the store falling within the transparent red circle would be considered near to the place field. Items delivered to stores falling within the transparent blue circle would be considered far from the place field. The radii of the circles emanating from the center of mass are determined by the length of the major axis of the place field (1 times the major axis and 2 times the major axis for near and far, respectively).

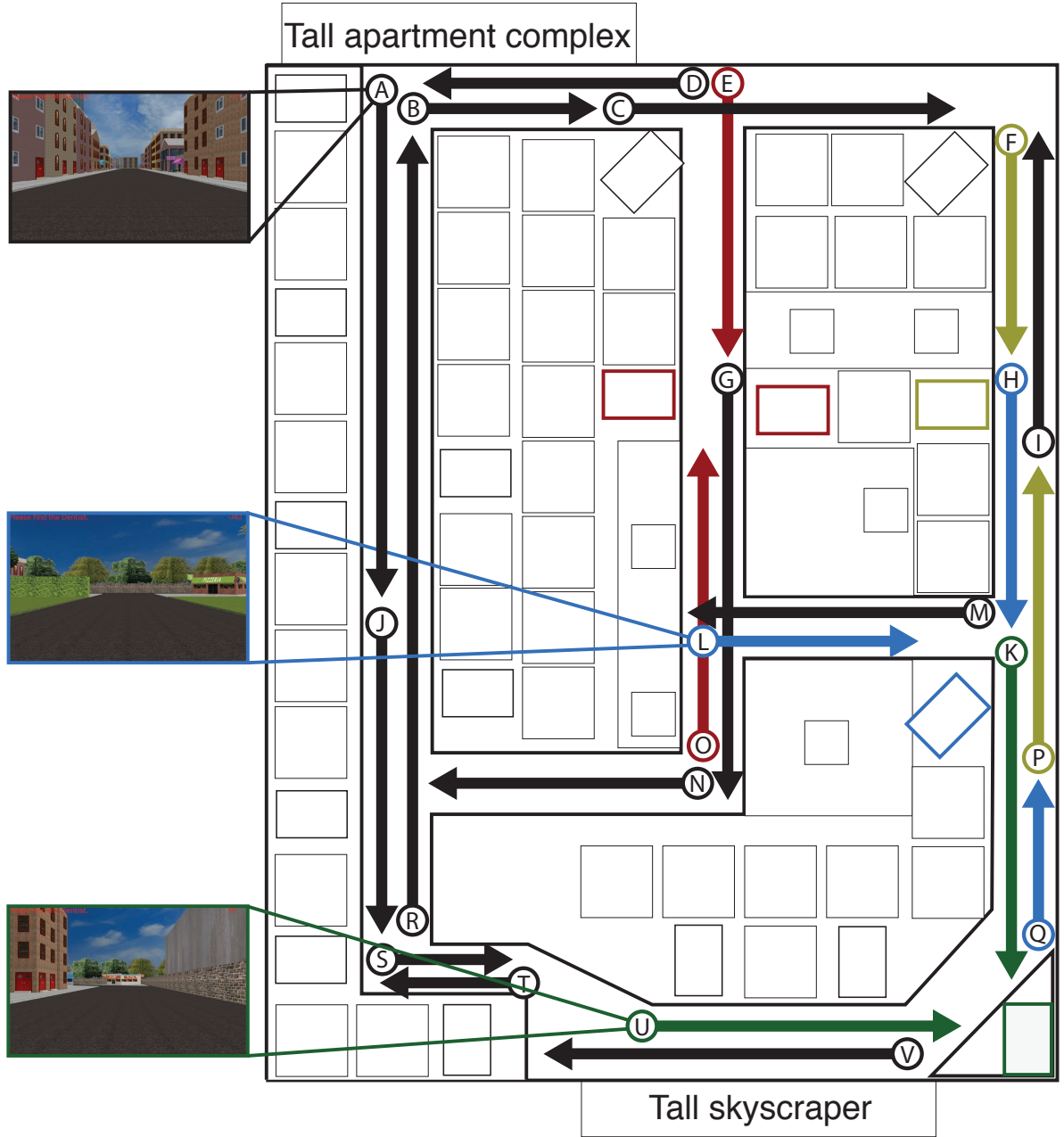


**Figure 2.7:** A visual representation of how the environment was divided into regions for the view-responsive cell analysis. Each arrow represents the area of the town and direction of travel for its respective region. Arrows with the same color (excluding black arrows, which are all distinct regions) shared a primary landmark, and thus were treated in the analysis as the same region (colored rectangles represent the landmark shared among these regions). For illustrative purposes, screenshots of three of the regions are shown on the left (regions A, L, and U, taken at the beginning (tail end) of their respective arrows). Note that the field of view during navigation was 60°, thus objects and landmarks immediately to sides of the current location are not visible.

## 2.5 Supplemental Tables

**Table 2.1:** Summary of place-responsive cell counts across subjects. The table shows the total number of cells and the total number of place-responsive cells for each recording session, aggregated by brain region (H: hippocampus, A: amygdala, EC: entorhinal cortex, PHG: parahippocampal gyrus, ANT: localization accuracy limited to anterior MTL). Sessions with less than four place-responsive cells were excluded from reinstatement analyses. Though session 1 of subject 1 had 11 identified place-responsive cells, it was excluded from the reinstatement analyses due to not having any valid recalls.

Subject #	Session	Trials	Region					Totals
			H	A	EC	PHG	ANT	
1	1	1	4 of 16	2 of 5	5 of 8	0 of 0	0 of 0	11 of 29
	2	1	5 of 26	0 of 4	5 of 11	0 of 0	0 of 0	10 of 41
	3	2	6 of 17	0 of 5	1 of 8	0 of 0	0 of 0	7 of 30
2	1	1	6 of 8	0 of 0	2 of 9	1 of 7	0 of 0	9 of 24
	2	3	0 of 0	0 of 0	4 of 11	0 of 7	0 of 0	4 of 18
	3	2	1 of 4	0 of 0	1 of 8	0 of 6	0 of 0	2 of 18
3	1	3	6 of 17	3 of 7	0 of 0	0 of 0	0 of 0	9 of 24
	2	3	4 of 10	1 of 4	0 of 0	0 of 0	0 of 0	5 of 14
	3	3	7 of 17	3 of 8	0 of 0	0 of 0	0 of 0	10 of 25
4	1	6	1 of 4	5 of 9	0 of 0	0 of 0	1 of 4	7 of 17
	2	8	0 of 1	3 of 7	0 of 0	0 of 0	1 of 2	4 of 10
5	1	6	1 of 12	0 of 8	1 of 8	0 of 0	0 of 0	2 of 28
6	1	4	1 of 10	0 of 2	0 of 0	0 of 0	1 of 14	2 of 26
	2	4	1 of 13	0 of 0	0 of 0	0 of 0	3 of 11	4 of 24
7	1	10	1 of 17	0 of 0	3 of 7	0 of 0	0 of 0	4 of 24
	2	8	4 of 17	0 of 0	1 of 2	0 of 0	0 of 0	5 of 19
Totals			48 of 189	17 of 59	23 of 72	1 of 20	6 of 31	95 of 371

**Table 2.2:** Place-responsive cells characteristics by subject and region. For each subject, only regions in which cells were recorded are included. The column “# Cells” shows the number of place-responsive cells recorded, out of the total number of cells. The column “FR (Hz)” shows the average firing rate within a region for all movement epochs during the task, regardless of location in the virtual environment. The column “In Field FR (Hz)” shows the average firing rate within a region within the cells’ place fields. The column “Field Size” shows the average size of the place fields within a region as a percentage of the traversable area of the virtual environment.

Subject #	Region	# Cells	FR (Hz)	In Field FR (Hz)	Field Size
1	Amygdala	2 of 14	0.18	0.54	2.64
	EC	11 of 27	2.09	3.60	2.59
	Hipp Body	8 of 31	0.82	2.94	2.76
	Hipp Head	7 of 28	0.32	0.89	2.77
2	EC	7 of 28	1.82	4.53	2.68
	Hipp Body	7 of 12	0.37	5.97	3.26
	PHG	1 of 20	0.39	4.48	5.43
3	Amygdala	7 of 19	0.63	2.38	2.47
	Hipp Head	17 of 44	1.28	2.62	2.41
4	Amygdala	8 of 16	4.07	5.64	2.43
	Hipp Head	1 of 5	0.23	0.82	2.37
	Anterior MTL	2 of 6	0.35	1.22	2.46
5	Amygdala	0 of 8	-	-	-
	EC	1 of 8	0.05	0.60	2.35
	Hipp Head	1 of 12	0.27	1.12	2.20
6	Amygdala	0 of 2	-	-	-
	Hipp Head	2 of 15	0.15	1.60	3.01
	Hipp Tail	0 of 8	-	-	-
	Anterior MTL	4 of 25	7.78	9.71	2.52
7	EC	4 of 9	1.31	2.32	2.90
	Hipp Body	4 of 21	6.13	7.87	2.52
	Hipp Head	1 of 13	3.89	5.38	2.37

## Chapter 3: Repeating spatial activations in human entorhinal cortex

Jonathan F. Miller, Itzhak Fried, Nanthia Suthana, & Joshua Jacobs  
*Current Biology*, 25(8): 1080–1085, 2015

### 3.1 Summary

The ability to remember and navigate spatial environments is critical for everyday life. A primary mechanism by which the brain represents space is through hippocampal place cells, which indicate when an animal is at a particular location [O’Keefe and Dostrovsky, 1971]. An important issue is understanding how the hippocampal place-cell network represents specific properties of the environment, such as signifying that a particular position is near a doorway or that another position is near the end of a corridor. The entorhinal cortex (EC), as the main input to the hippocampus, may play a key role in coding these properties because it contains neurons that activate at multiple related positions per environment [Bjerknes et al., 2014, Derdikman et al., 2009, Frank et al., 2000, Hafting et al., 2005, Solstad et al., 2008]. We examined the diversity of spatial coding across the human medial temporal lobe by recording neuronal activity during virtual navigation of an environment containing four similar paths. Neurosurgical patients performed this task as we recorded from implanted microelectrodes, allowing us to compare the human neuronal representation of space with that of animals. EC neurons activated in a repeating manner across the environment, with individual cells spiking at the same relative location across multiple paths. This finding indicates that EC cells represent non-specific information about location relative to an environment’s geometry, unlike hippocampal place cells, which activate at particular random locations. Given that spatial navigation is considered to be a model of how the brain supports non-spatial episodic memory [Bird and Burgess, 2008, Buzsáki and Moser, 2013, Eichenbaum and Lipton, 2008, Hasselmo, 2012], these findings suggest that EC neuronal activity is used by the hippocampus to represent the properties of different memory episodes [Buckmaster et al., 2004, Frank et al., 2000].

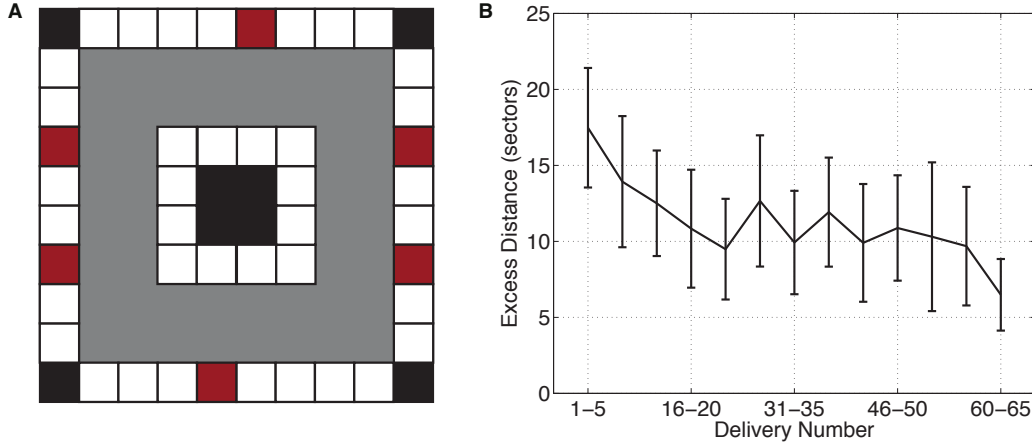


**Figure 3.1: Behavioral task and performance.** (A) An overhead schematic of the layout of the virtual environment. Red squares represent locations of the destination stores and white square are non-store buildings. Gray shading indicates regions of the environment where the patient could travel. (B) Subject average task performance as a function of delivery trial number. Performance is measured as the excess number of sectors traveled when searching for a destination store, compared to an ideal path. Error bars are 95% confidence intervals. See also Figure S1.

### 3.2 Results

We recorded 1,329 single neurons in various brain regions from 13 neurosurgical patients performing a virtual-navigation task. Patients were instructed to learn an environment’s layout and navigate between six destination “stores” as rapidly and accurately as possible. This environment was a square track (see Figure 3.1A), which limited the patients’ navigation path to particular regions of the environment. Navigation errors decreased across trials of the task (Figure 3.1B), indicating that patients successfully learned the environment’s layout.

Our main objective was to characterize how the spiking of individual neurons varied to represent the patient’s virtual spatial location. For each cell, we computed firing rate maps corresponding to the cell’s mean rate of spiking as a function of the current virtual location. A previous analysis of this dataset [Jacobs et al., 2010a] revealed many *path cells*, which coded for whether the participant was traveling clockwise or counterclockwise around the track. Thus, we computed firing rate maps separately for movements in clockwise and counterclockwise directions. We calculated these maps in a smoothed manner, as well as in a discretized manner that binned the patients’ location into one

of 25 sectors on each side of the track.

Next, we identified cells that significantly varied their firing rate according to the patient's virtual location. We used a one-way ANOVA as a screening procedure to identify individual neurons whose firing rates varied in response to the current sector of the environment. According to this measure, 313 cells (23.5%) were responsive to the location, a percentage that is in line with previous single-cell studies of human virtual navigation [Ekstrom et al., 2003, Jacobs et al., 2010a, 2013]. Our subsequent analyses focused on more precisely characterizing the activity of these cells.

A distinctive feature of some location-responsive cells in rodents is that they activate at multiple spatial locations that are related to each other, such as positions just before or after a curve [Frank et al., 2000], locations at particular distances from borders [Bjerknes et al., 2014, Derdikman et al., 2009, Solstad et al., 2008], or spots associated with particular landmarks [Hargreaves et al., 2005, Tsao et al., 2013]. We sought to identify analogous types of representations in humans by searching for cells that exhibited significant *path equivalence* across distinct sections of the virtual environment [Frank et al., 2000]. We computed the path-equivalence coefficient for each cell, which is a measure of the similarity of the cell's firing activity across two or more corridors (see *Experimental Procedures*). A cell that exhibited significant path equivalence is one that activated at the same relative position on multiple sides, such as a cell that spiked when a person was passing through the midpoint of any of the four paths. Of the 313 location-responsive cells, 30 (9.6%) exhibited significant path-equivalent firing patterns ( $p < 0.001$ ).

Three example path equivalent cells are shown in Figure 3.2. Figure 3.2A–C highlights one cell in the EC that activated consistently as the patient approached the end of each corridor during clockwise movement. Figure 3.2D–F shows a different cell in the EC that activated at similar locations across multiple corridors, with the locations of activations shifting between clockwise and counterclockwise movements. Figure 3.2G–I illustrates a cell from cingulate cortex that activated near the beginning of multiple corridors during counterclockwise movement. Additional example cells are shown in Figure 3.3.

We found significant levels of path-equivalent cells in only two regions: the entorhinal cortex and

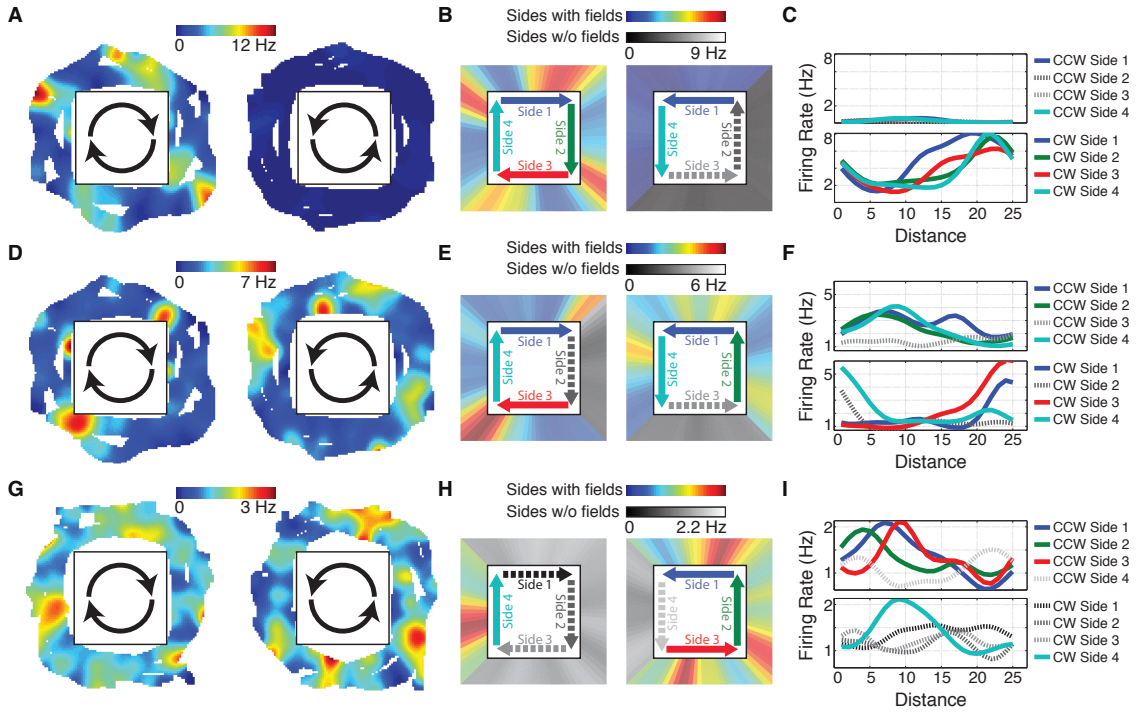


**Figure 3.2: Path equivalent cell firing rate maps.** **Top Row:** Activity of a cell in patient 2's entorhinal cortex. (A) Two dimensional firing rate map for epochs of clockwise (left) and counterclockwise (right) movement. (B) Linearized firing rate maps (smoothed with a 12-pt window) for epochs of clockwise (left) and counterclockwise (right) movement. Sides with regions of significantly elevated firing are shown in color, and sides without significant activations are in grayscale. (C) Firing rate as a function of distance from the beginning of the side, plotted separately for each side of the environment and for clockwise (bottom) and counterclockwise (top) directions. **Middle Row:** Activity of a cell in patient 2's entorhinal cortex. **Bottom Row:** Activity of a cell in patient 5's cingulate cortex. See also Figure S2.

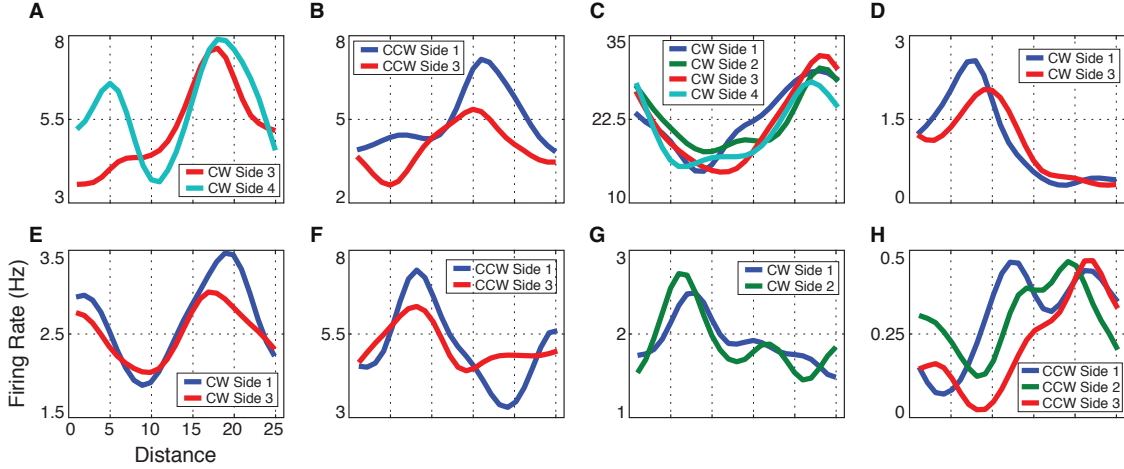


**Figure 3.3: Examples of path equivalent cells.** (A) A cell from patient 1's cingulate cortex during clockwise movement. (B) A cell from patient 2's entorhinal cortex during counterclockwise movement. (C) A cell from patient 2's entorhinal cortex during clockwise movement. (D) A cell from patient 5's entorhinal cortex during clockwise movement. (E) A cell from patient 10's parahippocampal gyrus during clockwise movement. (F) A cell from patient 12's entorhinal cortex during counterclockwise movement. (G) A cell from patient 13's hippocampus during clockwise movement. (H) A cell from patient 13's hippocampus during counterclockwise movement. See figure S3 for additional examples.

the cingulate cortex (Figure 3.4A). The magnitude of individual cells' path-equivalent firing was greater in EC compared to cingulate cortex, as indicated by the fact that the mean path-equivalence coefficient for EC path-equivalent cells (0.92) was greater than for path-equivalent cells in cingulate cortex (0.49;  $p < .05$ , rank-sum test). We specifically compared the level of path-equivalent activity between the hippocampus and its main input, the entorhinal cortex, and found that the entorhinal cortex contained more path-equivalent cells than the hippocampus ( $p < 0.05$ , post-hoc  $\chi^2$  test). This difference in the prevalence of path-equivalent cells cannot be attributed to a difference in the stability of the spatial coding between EC and hippocampus, as these two regions did not differ in the percentage of location sensitive cells that were stable over time (45% EC vs 53% hippocampus, n.s.). Prior research suggested functional differences across regions within the entorhinal cortex [Brun et al., 2008, Hafting et al., 2005, Hargreaves et al., 2005]. However, we did not find any difference in the proportion of path-equivalent cells between neurons located in the posterior vs. anterior EC, lateral vs. medial, or superior vs. inferior positions ( $\chi^2$  tests, all  $p$ 's  $> 0.1$ ).

The path-equivalence measure we employed is sensitive to the overall shape of a cell's firing pat-

tern. Thus, this measure could be influenced by cells with diffuse firing patterns [Quirk et al., 1992] rather than the spatially precise activations of conventional place or grid cells. To verify that the pattern of path-equivalent cells we observed was driven by the locations of peak spatial activations, we directly tested whether the relative locations of peak firing (place fields) were maintained across the sides of the environment. We identified each cell's place fields and then computed, for each cell, the percent of pairs of corridors of the environment where the relative locations of the place fields overlapped by at least 50% (Figure 3.4B). This analysis supports the finding that the EC plays a particular role in path equivalence because cells in EC had the greatest percent of corridors where place fields were located at the same relative location. Across all cells with place fields on two or more corridors in the EC, 40% of the possible corridor pairs had fields in overlapping locations. This is significantly more than the 22% of corridor pairs for cells in cingulate cortex ( $p < .05$ , ranksum test). If we restrict this analysis to only the previously identified path-equivalent cells, the difference is more pronounced (87% compared to 47%).

One possibility is that individual neurons do not represent particular locations but rather that these signals actually encode distance traveled. We compared the location- or distance-encoding hypotheses by comparing the firing patterns of neurons that exhibited place fields during both clockwise and counterclockwise directions. For the 25 path-equivalent cells that met this criterion, we computed the correlation between the mean clockwise and counterclockwise firing patterns. We distinguished distance and location-based firing by computing this correlation two ways: with the firing rate vectors aligned by absolute location, and with the vectors ordered by distance along the direction of movement. A positive correlation in the first case indicates location coding, whereas a positive correlation in the second indicates distance coding. Of the path-equivalent cells analyzed, 11 (44%) showed significant correlations. Of these 11, 8 showed distance coding (e.g., Fig. 3.2I), 1 showed location coding, and 2 were ambiguous. This result supports the hypothesis that some path-equivalent cells play a role in representing relative distance ( $p < .05$ ,  $\chi^2$  test).

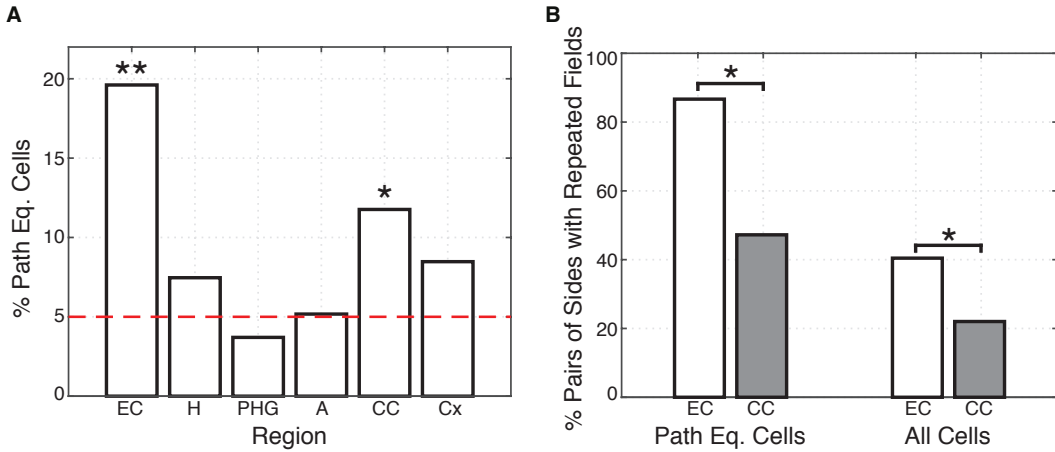


**Figure 3.4: Population measurements.** **(A)** Regional distribution of *path-equivalent cells*, which are location-responsive cells that have correlated responses across multiple corridors in the environment. EC: entorhinal cortex; H: hippocampus; PHG: parahippocampal gyrus; A: amygdala; CC: cingulate cortex; Cx: frontal/lateral-temporal cortex. **(B)** The percent of corridor pairs with place fields at the same relative locations. This measure is computed by identifying each cell with place fields on at least two corridors and measuring, across all pairs of corridors, how often place fields occur at the same relative location. \*\* denotes  $p < .0001$ , \* denotes  $p < .05$ . See also Figure S4 and Table S1.

### 3.3 Discussion

We examined human single-neuron recordings during virtual navigation and found a set of location-responsive cells that exhibited repeated firing patterns across multiple related areas of an environment. The key feature of these path-equivalent cells is that they consistently activated at the same relative position across separate corridors. This is the first evidence in humans that individual cells generalize features across multiple settings. By activating at multiple locations, these cells behave very differently from place cells, which activate at only one location per environment. Because path-equivalent cells are input to the hippocampus, it indicates that a critical function of the human hippocampus is to build distinctive neuronal representations from non-specific entorhinal input. An additional contribution of our work is showing that humans exhibit clear spatially modulated neuronal firing in *virtual* navigation, supporting the view that virtual and physical navigation are supported by some similar mechanisms, as previously demonstrated in rodents in various brain structures [Aghajan et al., 2014, Harvey et al., 2009, Ravassard et al., 2013].

Our demonstration of EC path-equivalent cells complements previous studies describing rodent neurons with repeating spatial firing patterns. One example is a study by Derdikman et al. [2009], which measured the activity of entorhinal grid cells as rodents navigated a constrained track. During movement in one direction of a hairpin maze, grid cells activated to represent equally spaced groups of locations that were consistently positioned across multiple corridors. As that paper demonstrates, grid cells generally reset their grids at entrances to individual corridors, giving rise to the appearance of a repeating pattern across different sections of the environment. Some of the cells in our study appear to exhibit a similar pattern, in which they reset their representation upon entering each corridor. This supports the view that the neural representation of space can be segmented by entrances to different compartments [Frank et al., 2000, Spiers et al., 2013].

Our findings are also related to data from Frank et al. [2000], who reported path-equivalent cells in rodent EC. The path-equivalent cells described in that study activated at analogous locations both within and across environments. Although several aspects of our findings are similar to the cells from that study, one critical difference is that when path-equivalent cells activate, the rat always has the same compass-like absolute heading. In contrast, for the path equivalent cells that we report, each activation corresponds to a circular heading and location within the environment. In a previous study from this dataset, we reported *path cells* that encoded direction in a circular manner such that they activated during either clockwise or counterclockwise movement [Jacobs et al., 2010a]. Thus, one possibility is that the entorhinal representation of direction in humans can be transformed according to an environment's layout so that it may depart from a fixed compass-like orientation scheme. Although human EC path-equivalent share features with grid cells, it is premature to conclude that the data reported here are from grid cells. As we demonstrate in *Figure S2*, owing to the four-way symmetry of our square environment, our data are not consistent with a grid cell that encoded the patient's position using a triangular coordinate system in two-dimensional space. We could not test whether the cells in our dataset exhibit grids aligned individual corridors [Derdikman et al., 2009] because the length of each corridor was too short to observe a possible grid repetition.

As studies of rodent spatial navigation characterize the functional relationship between different brain regions, theories of hippocampal function are converging on the idea that rodent spatial navigation is a model for studying other aspects of cognition, including episodic memory [Buzsáki, 2005, Buzsáki and Moser, 2013, Eichenbaum et al., 1999, Moser and Moser, 2013]. These theories share the idea that the representation of specific episodic memories can be considered analogous to the representation of locations by place cells. The role of the EC in this system may be to represent non-specific features of the behavioral setting [Hafting et al., 2005, Jacobs et al., 2010a, 2013, Sargolini et al., 2006, Solstad et al., 2008] for encoding into specific memories (or locations) by the hippocampus [Norman and O'Reilly, 2003]. During navigation, EC neurons may represent the attributes of a setting, with each cell activating at related locations, as in our findings and in some earlier animal work [Frank et al., 2000]. To our knowledge, our findings are the first demonstration of this type of featural neuronal coding in the human EC (cf. Mormann et al., 2008 [Mormann et al., 2008]). By demonstrating a key difference between hippocampal and entorhinal representations during navigation, our results support theoretical models regarding the diversity of information processing throughout the medial temporal lobe [Knierim et al., 2006, Norman and O'Reilly, 2003, Solstad et al., 2006].

### 3.4 Experimental Procedures

**Participants and Task Design.** The task design and methods for data acquisition are described in a previous study that examined this same dataset [Jacobs et al., 2010a]. All data analyses and results reported here are novel, although the prior study [Jacobs et al., 2010a] did qualitatively describe the activity of one cell we examined here. Thirteen patients undergoing surgical treatment for medication-resistant epilepsy participated in the study. All surgeries were performed by I.F. and the research protocol was approved by the University of California, Los Angeles Institutional Review Board. Patients played a 3D virtual navigation game on a laptop computer in their hospital room [Ekstrom et al., 2003, Jacobs and Kahana, 2010, Jacobs et al., 2010a, 2013]. The virtual environment consisted of six destination stores surrounding the perimeter of a square track, with the center of the environment obstructed by buildings (Figure 3.1A). On each delivery trial the patient transported

a passenger to their requested store destination as accurately as possible. After arrival at the destination, on-screen text displayed the name of the next randomly selected destination store.

**Electrophysiology.** We recorded spiking activity at 28–32 kHz using 40- $\mu\text{m}$  platinum-iridium microwire electrodes [Fried et al., 1999] connected to a Neuralynx recording system. Nine microwires extended from the tip of each clinical depth electrode. Action potentials were manually isolated using spike shape, clustering of wavelet coefficients, and interspike intervals [Quiroga et al., 2004]. We localized the locations of individual electrodes by co-registering post-operative CT scans with pre-implant MRI images and standardizing to a normalized brain [Talairach and Tournoux, 1988].

**Data Preprocessing.** We binned the firing rate of each cell into 100-ms epochs. We labeled each epoch with the patient’s location and direction of travel (either clockwise or counterclockwise around the square path). With the exception of the firing-rate maps presented in Figure 3.2A,D,G, all data analyses were conducted after linearizing patients’ location into 100 discrete sectors (25 per side) along the square path.

**Data Analysis.** For each cell, we computed a one-way ANOVA as a screening procedure to identify cells whose firing rate varied significantly according to environment sector, assessing significance with a shuffling procedure [Ekstrom et al., 2003]. To determine whether a cell displayed a similar firing patterns across multiple sides of the square track, we used a modified version of the path equivalence coefficient from Frank et al. [Frank et al., 2000]. The path equivalence coefficient is a measure of the degree to which a cell fires in similar relative locations on multiple trajectories. Only sides of the track that contained at least one region of three or greater contiguous sectors of elevated firing were included. We define the path-equivalence coefficient as the median correlation between the firing rates of all pairs of included sides minus the median correlation between the firing rates of all pairs of included sides and shuffled sides:

$$\text{median}(\text{corr}(\text{side}_i, \text{side}_j)) - \text{median}(\text{corr}(\text{side}_i, \text{shuf}_j))$$

where  $\text{side}$  is the firing rate of the corresponding 25 sectors,  $\text{shuf}$  is the firing rate of the corresponding 25 sectors shuffled as described below, and  $i$  and  $j$  range from 1 to the number of

included sides. To determine the firing rate values of a shuffled side, the corresponding firing rate values for the first half of that side were reversed and then the values of the two halves were swapped (e.g., a path of locations “A..BC..D” become “C..DA..B”). Statistical significance was determined using a permutation procedure (see *Supplemental Experimental Procedures*).

### 3.5 Supplemental Data

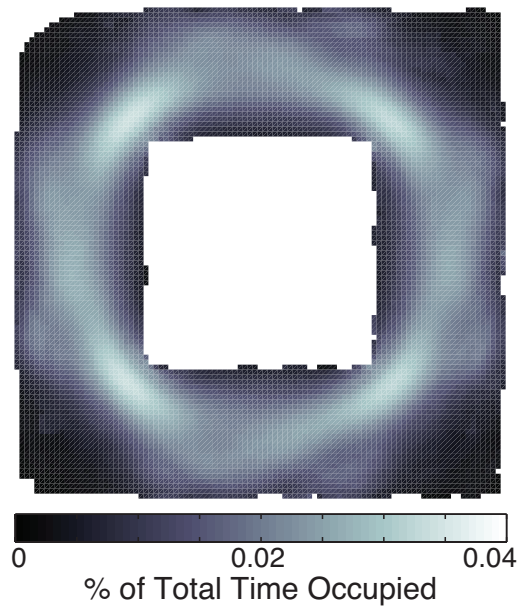


**Figure 3.5:** Average occupancy map across all sessions. Brighter shading represents a greater amount of time spent in the region.

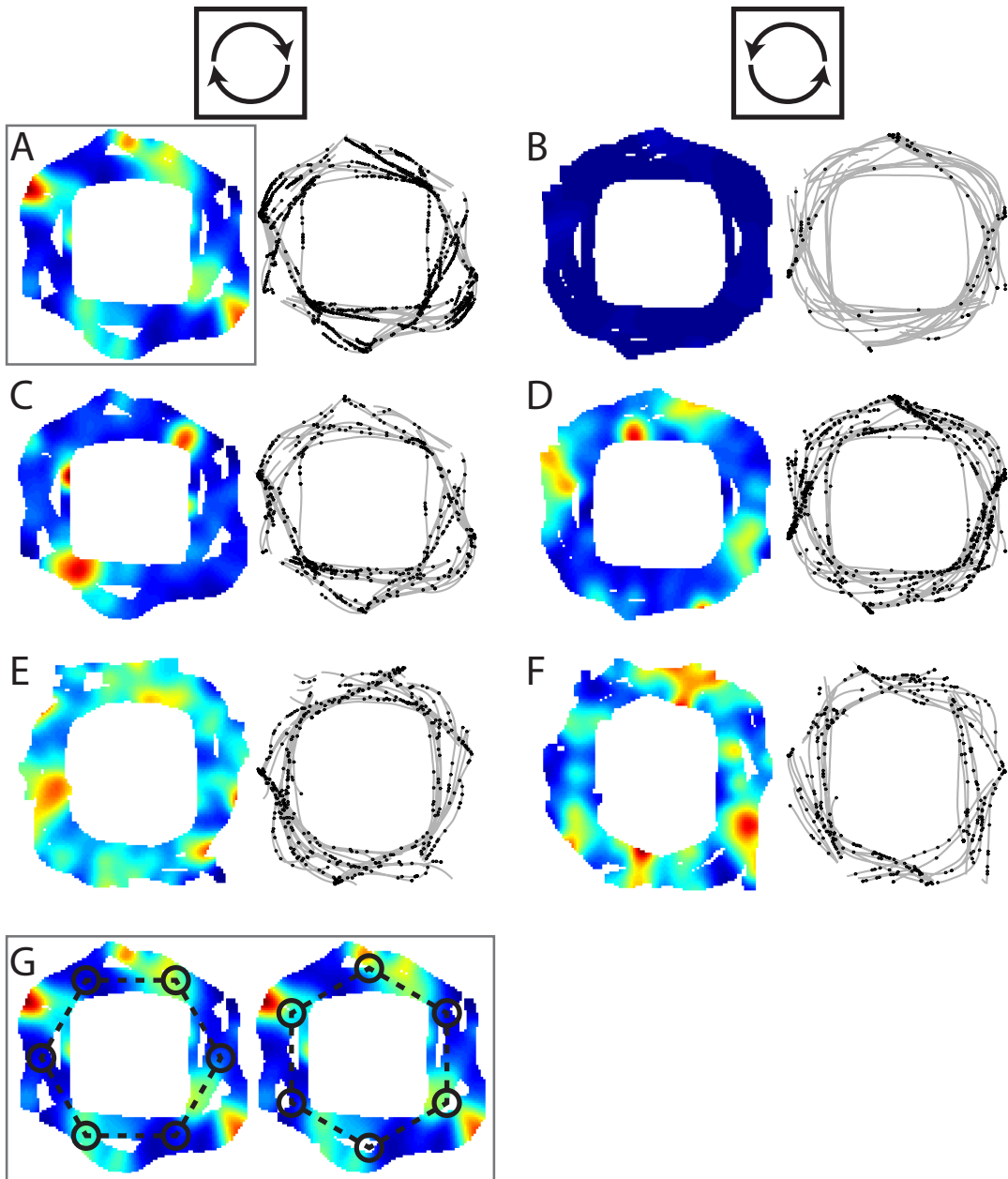


**Figure 3.6: Firing rate maps and associated spiking activity.** **A-F.** The rate maps from Figure 2 of the main text are replotted (left) along with the paths taken by the subject and locations where the cell fired, indicated by the gray lines and black dots, respectively (right). *A,C,E:* Clockwise activity for the cells shown in Figure 1. *B,D,F:* Counterclockwise activity for the cells shown in Figure 1. **G.** Firing rate map with an overlaid hexagon for a cell from patient 2's entorhinal cortex (as shown in panel A). The hexagon vertices do not closely fit the locations of the firing peaks, which suggests that our findings are not driven by a conventional grid cell that activates as if in an open arena. *Left:* Unrotated hexagon. *Right:* Hexagon rotated 30 degrees.

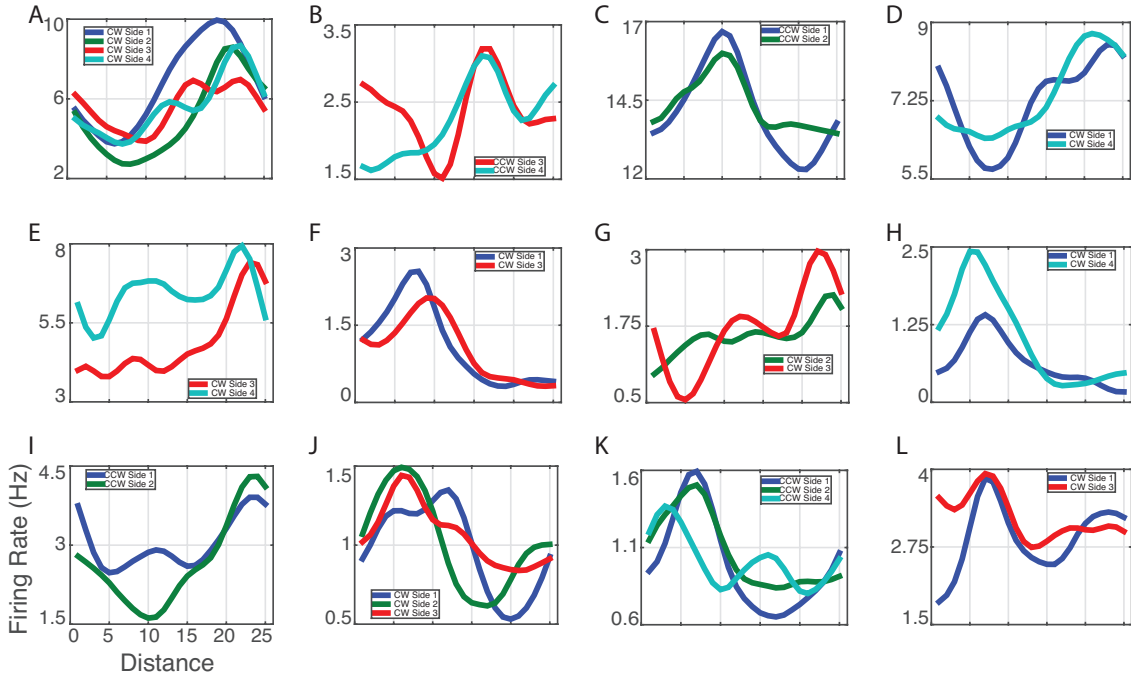
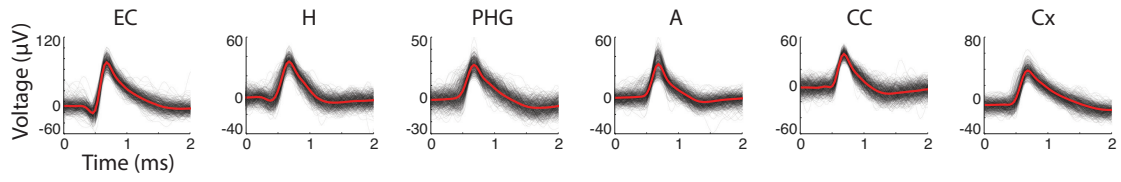


**Figure 3.7: Additional examples of path equivalent (PE) cells.** (A) A PE cell from patient 2. (B) A PE cell from patient 3. (C) A PE cell from patient 3. (D) A PE cell from patient 4. (E) A PE cell from patient 4. (F) A PE cell from patient 5. (G) A PE cell from patient 6. (H) A PE cell from patient 6. (I) A PE cell from patient 9. (J–K) One PE cell from patient 10 during two different directions of movement. (L) A PE cell from patient 11.



Region	Mean Firing Rate (Hz)	Firing Rate 5%-95% Range (Hz)	Mean Spike Amplitude (μV)	Background noise (μV)	Mean False Positive Rate	FP below 10%	FP below 20%	Mean False Negative (FN) rate	FN below 10%	FN below 20%
Entorhinal Cortex	4.0	0.1-11.9	44.8	6.8	3.7%	91.1%	95.6%	4.2%	88.6%	94.9%
Hippocampus	2.5	0.1-10.3	42.8	6.7	3.5%	87.0%	96.8%	3.7%	87.7%	95.4%
Parahippocampal Gyrus	2.0	0.1-7.6	36.8	6.1	2.0%	95.7%	97.9%	2.6%	94.7%	95.7%
Amygdala	2.7	0.2-9.7	51.9	6.7	7.6%	77.8%	88.3%	7.5%	77.1%	88.3%
Cingulate Cortex	4.1	0.2-11.8	45.0	8.0	6.7%	79.1%	89.8%	7.4%	76.7%	86.4%
Frontal/Temporal Cortex	3.2	0.2-11.2	42.3	6.9	5.0%	80.3%	92.2%	5.1%	80.3%	91.9%

**Figure 3.8:** Spike cluster characteristics. **Top:** Example spike waveforms from each brain region. Red line indicates the mean **Bottom:** Spike cluster isolation metrics. False-positive rate indicates the estimated percentage of spikes that were inappropriately designated as belonging to a given neuron. False-negative rate indicates the percentage of spikes that were caused by a given neuron but were inappropriately labeled as belonging to neighboring neurons or noise. We compared the spike waveforms of path-equivalent cells with those of other neurons and did not find any differences in their mean amplitude (41 μV for path-equivalent cells vs. 45 μV for other cells;  $p > 0.35$ , ranksum test) or in our false-positive or false-negative rates in distinguishing their waveforms from neighboring cells ( $p$ 's > 0.1, ranksum tests).

**Table 3.1:** Summary of path equivalent cells by patient and brain region. Counts indicate the number of path equivalent cells out of the total number of location-responsive cells. Numbers in parentheses indicate the total number of cells recorded, regardless of whether a cell was location-responsive. EC: entorhinal cortex; H: hippocampus; PHG: parahippocampal gyrus; A: amygdala; CC: cingulate cortex; Cx: frontal/lateral-temporal cortex.

Subject #	EC	H	PHG	A	CC	Cx
1	0 of 0 (0)	0 of 5 (12)	0 of 0 (0)	0 of 3 (20)	1 of 5 (18)	0 of 5 (28)
2	5 of 18 (38)	0 of 6 (27)	0 of 0 (4)	0 of 0 (0)	0 of 9 (40)	0 of 10 (52)
3	0 of 3 (12)	0 of 0 (3)	0 of 0 (0)	0 of 16 (74)	0 of 8 (14)	2 of 10 (47)
4	1 of 6 (32)	1 of 11 (39)	0 of 0 (0)	1 of 5 (39)	2 of 13 (35)	0 of 0 (21)
5	2 of 10 (34)	0 of 7 (45)	0 of 0 (0)	0 of 0 (0)	2 of 7 (38)	0 of 8 (51)
6	1 of 9 (24)	0 of 0 (0)	0 of 0 (0)	1 of 2 (13)	1 of 5 (37)	1 of 10 (32)
7	0 of 0 (0)	0 of 5 (24)	0 of 3 (5)	0 of 7 (23)	0 of 2 (5)	0 of 5 (17)
8	0 of 0 (0)	0 of 6 (39)	0 of 5 (27)	0 of 0 (1)	0 of 0 (0)	0 of 0 (7)
9	0 of 0 (0)	0 of 2 (8)	0 of 0 (0)	0 of 1 (2)	0 of 0 (0)	1 of 3 (9)
10	0 of 0 (0)	1 of 5 (15)	1 of 9 (24)	1 of 9 (28)	0 of 0 (0)	0 of 0 (6)
11	0 of 0 (0)	0 of 6 (26)	0 of 3 (4)	0 of 4 (12)	0 of 2 (19)	1 of 3 (37)
12	1 of 2 (8)	0 of 1 (12)	0 of 3 (22)	0 of 8 (40)	0 of 0 (0)	0 of 0 (0)
13	0 of 3 (10)	3 of 13 (35)	0 of 4 (8)	0 of 3 (14)	0 of 0 (0)	0 of 5 (13)
Total	10 of 51 (158)	5 of 67 (285)	1 of 27 (94)	3 of 58 (266)	6 of 51 (206)	5 of 59 (320)

### 3.6 Supplemental Experimental Procedures

**Participants.** The task design and methods for data acquisition were described in a previous study that examined this same dataset [Jacobs et al., 2010a]. In brief, thirteen patients undergoing surgical treatment for medication-resistant epilepsy participated in the study. All surgeries were performed by I.F. and the research protocol was approved by the University of California, Los Angeles Institutional Review Board. Our dataset is comprised of 35 individual testing sessions (30–50 minutes each), with each participant contributing between one and four sessions. All data analyses and results reported here are novel, although the prior study [Jacobs et al., 2010a] did qualitatively describe the activity of one cell we examined here.

**Behavioral Task.** Patients played a virtual navigation game [Ekstrom et al., 2003, Jacobs et al., 2010a, 2013] on a laptop computer in their hospital room. The virtual environment consisted of six destination stores surrounding the perimeter of a square track, with the center of the environment obstructed by buildings. Patients traveled either clockwise or counterclockwise around the track. Two stores each were located on the east and west walls (sides 2 and 4), and one store each was

on the north and south walls (sides 1 and 3). The stores were all visually distinct. The patients navigated the environment using a game controller. On each delivery trial the patient transported a passenger to their requested store destination as accurately as possible. After arrival at the destination, on-screen text displayed the name of the next randomly selected destination store.

**Electrophysiology.** We recorded spiking activity at 28–32 kHz using 40- $\mu$ m platinum-iridium microwire electrodes [Fried et al., 1999] connected to a Neuralynx recording system. Nine microwires extended from the tip of each clinical depth electrode. The first eight wires were insulated except for their tip and were used to record action potentials. The ninth microwire had its insulation stripped for  $\sim$ 1 cm and served as the voltage reference for the other wires. Action potentials were manually isolated using spike shape, clustering of wavelet coefficients, and interspike intervals [Quiroga et al., 2004]. We localized the locations of individual electrodes by co-registering post-operative CT scans with pre-implant MRI images and standardizing to a normalized brain [Talairach and Tournoux, 1988]. Assessing entorhinal subregions is an area of ongoing research [Khan et al., 2014]. The approach we used to localize within the EC was by performing median splits across extent of our EC electrodes in the lateral/medial, anterior/posterior, and ventral/dorsal axes.

**Data Preprocessing.** We binned the firing rate of each cell into 100-ms epochs. We labeled each epoch with the patient’s location and direction of travel (either clockwise or counterclockwise around the square path). Following previous work on this dataset [Jacobs et al., 2007, 2010a], epochs without movement and epochs where clockwise or counterclockwise direction was not defined (i.e., when facing towards or away from the center of the environment) were excluded from analysis. With the exception of the firing-rate maps presented in Figure 2A,D,G, all data analyses were conducted after linearizing patients’ location along the square path.

**Environment Linearization.** We linearized the paths of the environment by mapping the angle of every (x,y)-coordinate pair into 1 of 100 sectors, with the width of each sector equal to 3.6°. We used this angular binning scheme because patients’ generally followed a circular path during navigation (Figure S1). When viewed in an overhead map, a linearized location value of 1 corresponds

to the top-left corner of the environment. Values increase in a clockwise direction around the square path (thus, sectors 1–25 correspond to the top corridor, sectors 25–50 to the right, sectors 51–75 to the bottom, and sectors 76–100 to the left). After linearizing the location, we computed linearized firing rate maps separately for all epochs of clockwise movement and all epochs of counterclockwise movement. Linear firing rate maps were circularly convolved with a 6-sector gaussian window before data analyses.

**Location-responsive cells.** For each cell, we computed a one-way ANOVA as a screening procedure to identify cells whose firing rate varied significantly according to environment sector [Ekstrom et al., 2003]. We separately validated (data not shown) that the outcome of this ANOVA approach is very similar to the information theoretic approaches used by previous studies for this purpose [Markus et al., 1994]. We created a distribution of 1000 p-values, each of which was the result of performing the ANOVA on shuffled firing rate maps, whereby the firing rate of the cell was circularly shifted by a random amount relative to the behavioral epochs. In order for a cell to be considered location-responsive, the p-value resulting from the unshuffled data must have been less than 900 of the p-values calculated using the randomly time-shifted data. We performed these calculations separately for epochs of clockwise and epochs of counterclockwise travel. A cell was considered spatially responsive if the true p-value met this criteria for either direction of travel. Note that this screening ANOVA merely identifies cells whose firing rates vary systematically according to location, which is not the same as identifying bona fide place cells, as was performed on this dataset by Jacobs et al. (2010).

**Path Equivalent Cells.** To determine whether a cell displayed a similar firing patterns across multiple sides of the square track, we used a modified version of the path equivalence coefficient from Frank et al. [Frank et al., 2000]. The path equivalence coefficient is a measure of the degree to which a cell fires in similar relative locations on multiple trajectories. Only sides of the track that contained at least one region of three or greater contiguous sectors of elevated firing were included. In this way, our analyses focused on characterizing the specific locations where individual neurons activated,

leaving future studies to examine the important issue of why some cells show diminished firing in areas of certain environments. We define the path-equivalence coefficient as the median correlation between the firing rates of all pairs of included sides minus the median correlation between the firing rates of all pairs of included sides and shuffled sides:

$$\text{median}(\text{corr}(\text{side}_i, \text{side}_j)) - \text{median}(\text{corr}(\text{side}_i, \text{shuf}_j))$$

where *side* is the firing rate of the corresponding 25 sectors, *shuf* is the firing rate of the corresponding 25 sectors shuffled as described below, and *i* and *j* range from 1 to the number of included sides. To determine the firing rate values of a shuffled side, we followed the shuffling method of Frank et al. (2000) in which the firing rate values for the first half of the side were reversed and then the values of the two halves were swapped (sequence “A..BC..D” would become “C..DA..B”).

To determine whether a cell’s path equivalent coefficient value was greater than chance, we created a null distribution of 1000 path equivalent coefficients calculated on permuted data. For each permutation, we circularly shifted the 25 firing rate values of each included side by a random amount, independently for each included side, and recalculated the path equivalent coefficient. If the true coefficient was greater than the 95<sup>th</sup> percentile of coefficients calculated on shuffled data, then that coefficient was deemed to be significant at  $p < 0.05$ . This procedure was done twice, one for clockwise movements and one for counterclockwise. If the path equivalent coefficient for either direction of movement was significant, then the cell was classified as a path equivalent cell.

**Place field analyses.** We also used a shuffling procedure to identify the specific regions of the environment that exhibited significantly elevated firing rates (“place fields”) for each cell. For a given cell and circular direction of travel we created a set of 1,000 shuffled firing rate maps, whereby the firing rate of the cell was circularly shifted by a random amount relative to the behavioral epochs. The firing rate within a sector was considered elevated if the activity from the unshuffled data was greater than the 90<sup>th</sup> percentile of the firing rates for that sector from the shuffled data.

To quantify how often a single cell’s place fields appeared at the same relative location on different sides of the path, we computed, for each cell, the degree of relative overlap of each pair of fields. We counted a pair of fields as overlapping if their relative position along each corridor overlapped by at

least 50%. To ensure the results were unbiased for each cell, we limited the analysis to only sides with place fields, and divided the number of overlapping pairs by the total number of possible pairs (i.e., pairs of sides with place fields). Counts were combined across clockwise and counterclockwise directions.

In the phenomenon of rate remapping, a cell distinguishes between different spatial representations via variations in the absolute firing rate levels [Allen et al., 2012, Leutgeb et al., 2005a, Quirk et al., 1992, Singer et al., 2010]. We tested whether cells we observed exhibited a related phenomenon in which they varied their firing rates across different fields. For each cell that exhibited two or more fields at the same relative location on different sides of the track (118 cells), we performed an ANOVA comparing the firings rates from when the patient occupied those fields. 8 of these cells (6.8%) significantly varied their firing rates between related fields. This level is not significantly greater than chance (5%) and thus not indicative of rate remapping.

The task's virtual environment exhibits reflective symmetry in that opposite corridors have similar store layouts. There is one store on the east and west corridors and two stores on the north and south corridors (Figure 1A). Given this layout, it was possible that a neural signal related to the quantity or location of nearby stores could masquerade as exhibiting path-equivalence between opposite walls of the environment. We were interested in testing the possibility that path equivalence is related to the presence of nearby landmarks rather than the environment's overall spatial geometry. For each cell with place fields on exactly two sides, we calculated how often the place fields were positioned on opposite versus neighboring sides. This comparison was important because if two place fields appeared on opposite sides, then they could be driven by the identical store layouts between these areas. In contrast, if place fields were not related to stores, the percent of cells with fields on opposite sides would be at the chance level of 33%. In line with this prediction, 32% of the cells with two place fields had these fields positioned on opposite sides. We separately performed this analysis for cells from each brain region, with no region's percentage significantly differing from chance levels (all  $p$ 's > 0.1).

**Clockwise/Counterclockwise comparison.** For each path-equivalent cell, we classified the relationship between the cell’s clockwise and counterclockwise firing patterns as either coding relative distance from the start of a corridor, coding absolute location, no relationship, or an ambiguous relationship. We only included cells with at least one place field in both directions of travel, and we only included corridors with a place field. For each included cell, we performed two correlations. First, we correlated mean clockwise activity and mean counterclockwise activity directly such that a significant positive correlation indicates the encoding of location. We then correlated mean clockwise and mean counterclockwise activity with the counterclockwise vector reversed, such that the first position in each vector follows the direction of movement to always represent the corridor’s entry point. A significant positive correlation here indicates that a neuron encodes relative distance rather than location. If we observed a significant correlation in both cases (due, for example, to place fields in the middle of the corridors), we classified the relationship as ambiguous.

## Chapter 4: Human hippocampal theta and its relationship to speed, memory, and voluntary movement

Jonathan F. Miller, Michael Sperling, Ashwini Sharan, Kathryn Davis, Joel M. Stein, Sandhitsu R. Das, & Joshua Jacobs

### 4.1 Abstract

In rodents, the power and frequency of the hippocampal theta rhythm (4-8 Hz) is strongly modulated by ongoing behavior, particularly movement and running speed. In contrast, human hippocampal theta appears to be more intermittent, and its relationship to movement is not well characterized. Electrocorticographic (ECOG) recordings from human hippocampus have shown increases in low frequency power associated with periods of virtual movement compared to periods of stillness, yet these previous tasks were not designed to explicitly examine the effects of movement speed nor were they designed to encourage patients to pay continuous attention to their virtual location. By systematically modulating speed of movement and memory demands, our task encourages patients to attend to their moment-by-moment position in the environment, thereby optimizing the task to elicit movement related low frequency activity. In addition, theta power in human hippocampus has been shown to be both positively and negatively correlated with memory performance. Using data from neurosurgical patients with depth electrodes specifically localized to the hippocampus, we sought to untangle this complex relationship between low frequency oscillatory power, movement speed, and memory performance by employing a multivariate statistical approach. We provide evidence that movement related theta oscillations in human hippocampus reliably appear at frequencies between 1-4 Hz and increase in power as movement speed increases. We also find that memory related low frequency oscillations at distinct frequencies distinguish between better or worse memory performance, such that activity at ~3 Hz is associated better memory, and activity at ~7 Hz is associated with worse memory. Together, we show that movement related theta activity appears at lower frequencies in human hippocampus than in rodents, and that memory related theta activity

has dissociable effects based on the precise frequency, helping to resolve the conflicting literature concerning the role of human hippocampal theta in memory function.

## 4.2 Introduction

The hippocampus has been implicated as playing a vital role in both memory and spatial navigation across a wide range of mammalian species. In rodents, where hippocampally dependent behavior and its underlying physiology have been studied most intricately, theories that attempt to explain hippocampal function often rely on the theta rhythm. The theta rhythm, a large-amplitude oscillation generally defined as occurring in the 4–8 Hz range (though sometimes as low as 3 or as high as 12 Hz [Hasselmo and Stern, 2014, Kramis et al., 1975]), has close functional ties to a broad range of behaviors and processes, including arousal [Sainsbury et al., 1987], voluntary movement such as whisking [Semba and Komisaruk, 1984], jumping [Lenck-Santini et al., 2008], or running [Vanderwolf, 1969], and memory function [Winson, 1978]. In fact, the theta oscillation has been closely linked to so many ongoing behaviors that it has been described simply as the “on-line state of the hippocampus” [Buzsáki, 2002].

Given its high amplitude and consistent behavioral role in the rodent, it is thus surprising that theta is observed only intermittently in human hippocampus, and its relationship to behavior is much less well understood. For instance, in rodents, hippocampal theta is strongly associated with voluntary movement, and the amplitude of theta is positively correlated with movement speed [Hinman et al., 2011, McFarland et al., 1975]. However, human studies show that hippocampal theta, though present, appears only transiently and for relatively short durations during movement conditions [Ekstrom et al., 2005, Kahana et al., 1999, Watrous et al., 2013]. Furthermore, though the positive relationship between theta amplitude and movement speed has been observed in humans [Watrous et al., 2011], this result has neither been replicated nor studied in a task where speed of movement was carefully controlled and attentiveness to current location in the environment was more explicitly encouraged.

Similarly, the role of theta in supporting learning and memory is well established in rodents, and theta is associated with the ability to accurately learn and navigate throughout an environment.

Hippocampal place cells, which fire action potentials when the rodent is located at a particular location in the environment, spike at distinct phases of individual theta cycles [O’Keefe and Recce, 1993, Skaggs et al., 1996], and disruption of the theta rhythm strongly impairs performance on spatial learning tasks such as the Morris water maze [McNaughton et al., 2006b]. In contrast, findings on the role of human theta with regard to learning and memory are somewhat conflicting, with certain subsets of studies reporting that theta is associated with good memory performance [Klimesch et al., 1996, Lega et al., 2012, Sederberg et al., 2003] and others reporting a lack of relationship or indeed that theta associated with poor performance [Burke et al., 2013, Guderian et al., 2009, Long et al., 2014b, Sederberg et al., 2007]. These opposing findings cast doubt on assumptions that rodent-derived theories of hippocampal function translate to other species, particularly to primates and humans.

The present study was designed to overcome limitations of previous work that attempted to examine the correspondence, or lack thereof, between human and rodent hippocampal theta. In our virtual reality (VR) task, we systematically vary movement speed in order to ensure a wide distribution of speed parameters, enabling us to investigate the theta/speed relationship on a more detailed level than previously possible. In addition, because of the variations in speed and memory demands, our task is designed to encourage participants to carefully and continuously attend to their present location in the environment, with the goal of eliciting more reliable movement related neural activity than past VR studies of human navigation.

To investigate how neural activity varied as a function of movement conditions and memory performance, we examined electrocorticographic (ECoG) activity from hippocampal depth electrodes implanted in neurosurgical patients as they performed a spatial learning and memory virtual-reality game. Our task was optimized to (1) elicit movement-related theta oscillations in humans by encouraging participants to carefully attend to their moment-by-moment location in the virtual world; (2) to examine the effect of movement speed, as well as automatic vs manually controlled movement, on hippocampal oscillations by comprehensively collecting data from a wider range of speeds than in previous studies; and (3) to examine the relationship of hippocampal oscillations and memory

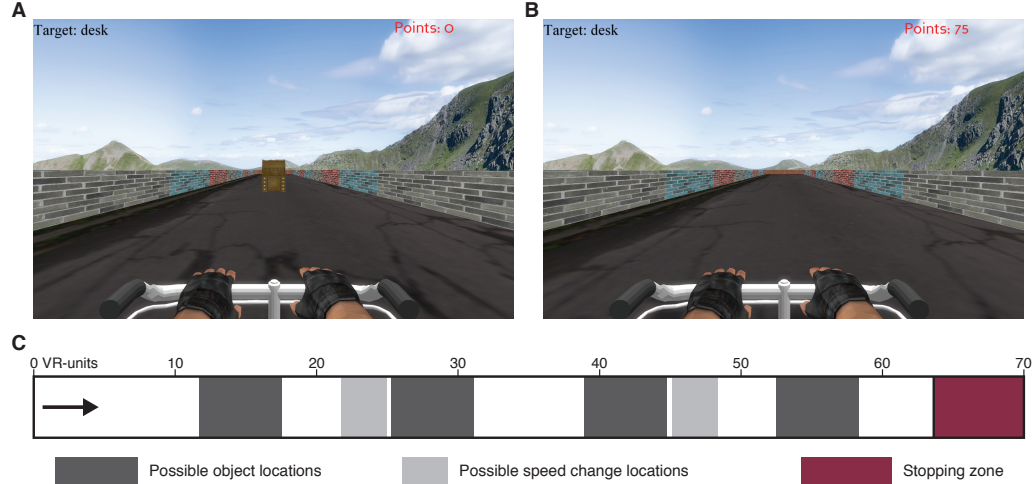


**Figure 4.1: Behavioral task methods.** **A.** A screenshot of the task, taken during a learning trial with the target object visible. **B.** A screenshot of the task, taken after the learning trials with the target object invisible. Patient's must press the button when they think they are at the invisible object's location. **C.** An overhead schematic of the task. The arrow represents the starting point of each trial. Potential object locations are shown in dark grey, potential regions where speed may change are shown in light grey, and the end of the track where patient's must press the button is shown in red.

performance through the use of a location-memory task embedded within the virtual environment, allowing us to distinguish oscillatory activity related to movement oscillatory activity related to memory function. Furthermore, by using newly developed brain imaging techniques, we ensure that all electrodes included in the dataset are truly within the hippocampus proper.

### 4.3 Methods

**Participants** Nine participants undergoing treatment for medication-resistant epilepsy participated in the study. Patients were implanted with depth electrodes for the purpose of functional mapping and the localization of seizure focus. The implantation sites were determined solely by clinical concerns, though electrodes were often placed in medial temporal lobe regions that are of interest experimentally. Data were collected at Thomas Jefferson University Hospital (TJU; Philadelphia, PA) and the Hospital of the University of Pennsylvania (HUP; Philadelphia, PA). Research protocols were approved by the institutional review boards at each participating hospital, and informed consent was obtained from all participants.

**Experimental Paradigm** The aim of our experimental design was to encourage patients to pay continuous attention to their location in the virtual environment, with the goal of eliciting more reliable hippocampal activity than seen in previous studies of human navigation. Due to constraints of the clinical environment, patients must perform experimental tasks on a laptop computer in their hospital room. In order to make current location in the environment a salient feature of the task, we asked patients to press a button on their game controller when they were at the location of a hidden object, while simultaneously manipulating speed of movement. During the 3D virtual spatial memory game, patients were moved from the beginning to the end of a 70 virtual reality (VR) unit long track. The ground was textured to mimic asphalt, and the track was surrounded by stone walls (See Figure 4.1). On each trial, patients were placed at the beginning of the track facing directly along the long axis. Patients initiated the beginning of the trial by pressing a button on a game controller. Once initiated, a four second long countdown was displayed. After the countdown, patients were moved forward along the track. Within each third of the track, patients were moved at a constant speed chosen uniformly from the range of 2 VR-units/second up to a maximum of 12 VR-units/second. Locations where speed changes began are indicated by the light gray shading in the schematic shown in Figure 4.1C. Between speed segments, speed was ramped up or down for one second to avoid a jarring transition between speeds.

While moving, the patients' goal was to learn the location of a hidden object. The first two times that the patient traveled down the track, the object's location was visible (Figure 4.1A). On subsequent trials, the object was invisible, and patients were instructed to press the button on the controller when they believed they were at the correct location (Figure 4.1B). The closer the patient pressed the button to the correct location, the more points they received (as indicated in the top right of the display), thus encouraging careful attention to current location in the environment. The error, or response accuracy, between the true location of the object and the button press provides us with a continuous measure of memory performance. Patients were also required to press the button when they approached the end of the track where the ground was colored red. Patients saw four different objects – 16 trials of each – over the course of a session, with each object located at a

different randomly selected location. Possible object locations are indicated by the dark gray shading in Figure 4.1C. Unlike most previous studies of human spatial navigation, the present study moves patients without active input so that we can carefully manipulate movement speed. To investigate whether there is a distinction between manually or automatically controlled movement, patients were not moved automatically down the track on 25% of trials, but rather controlled their own forward movement using the joystick on the game controller.

**Electrophysiological Recordings** Electrocorticographic (ECoG) data were recorded from implanted depth electrodes via the clinical recording systems present at the participating hospitals (Nihon Kohden, TJU; XLTEK, HUP). Data were recorded at a sampling rate of either 1000 or 500 Hz. Data were initially referenced to common intracranial or scalp contact, and were subsequently re-referenced using an anatomically weighted referencing scheme prior to analysis. Data were notch filtered at 60Hz using a zero phase distortion Butterworth filter to remove line noise prior to subsequent analyses. ECoG recordings were aligned to the behavioral task laptop via synchronization pulses sent to the clinical recording system.

**Electrode Localization** For patients 1 and 2, depth electrodes were localized manually by a neuroradiologist using post-operative MRIs, and subfield level information was not obtained. For patients 3 through 7, a fully automated multi-atlas volume segmentation algorithm [Yushkevich et al., 2015] applied to the T2-weighted scans defined medial temporal lobe regions, including hippocampal subfields (CA1, CA2, CA3, and dentate gyrus), entorhinal cortex, perirhinal cortex, and parahippocampal cortex. Contact coordinates were then mapped from the CT to MRI space and anatomic locations of the contacts automatically generated according to the volume segmentation. A neuroradiologist reviewed and confirmed depth electrode localizations based on the co-registered source images and the processed data.

**Oscillatory Power** For each trial, beginning with the start of movement and terminating when the patient pressed the button at the end of the track, we computed spectral power by convolving the voltage time series with Morlet wavelets (wave number 7) at 80 logarithmically spaced frequencies

between 1 and 128 Hz. To account for changes in baseline power across sessions, we normalized the power at every frequency by computing the  $Z$ -transformed power relative to the mean and standard deviation of a recording period taken just prior to the start of the experimental session.

In order to characterize the effect of speed changes on oscillatory power, we computed spectral power for each trial, as described above. We then clipped the power time series beginning 250 ms before a speed change occurred until 2000 ms after the initiation of the speed change. For each clip, we normalized the power based on the mean and standard deviation of the 250 ms pre-speed change interval. In addition, given the proximity of the third speed change to the end of the track, only the first two speed changes of each trial were used.

In order to quantify how the instantaneous oscillatory frequency varied with behavior, we used a peak-picking procedure to calculate the peak oscillatory frequency for every trial [Lega et al., 2012]. To do so, we first calculated spectral power by convolving the voltage time series with Morlet wavelets (wave number 7) at 80 logarithmically spaced frequencies between 1 and 12 Hz. We used a robust regression in log-space to isolate the  $1/f$  background power spectrum [Miller et al., 2007] for each trial, and we subtracted this baseline measure from original power spectrum. To identify narrowband peaks, we identified local maxima in the corrected signal that exceeded two standard deviations above the  $1/f$  background.

**Regression Analysis** We used a multivariate approach to capture the relationship of oscillatory signals to the experimental/behavioral variables. For every trial, we averaged across time to produce an estimate of the mean power at each frequency. In addition to mean power, we also computed (1) average speed, and (2) response accuracy. Our multivariate linear model took the following form, computed separately for each frequency ( $f$ ) and hippocampal electrode ( $e$ ):

$$ZPower_{(f,e)} = \beta_{0(f,e)} + \beta_{1(f,e)}^{Speed} + \beta_{2(f,e)}^{Mem} + \beta_{3(f,e)}^{Auto} + \beta_{4(f,e)}^{tNum} + \epsilon \quad (4.1)$$

where  $ZPower$  is the average power at the frequency and electrode,  $Speed$  is the average speed during the trial,  $Mem$  represents the behavioral performance on the trial in terms of distance error,

*tNum* is the count of the trial within a given session, and *Auto* indicates whether trial was an automatic movement trial or a manually controlled movement trial. We normalized each predictor variable between the range of zero and one.

For each frequency and predictor variable, we obtained a distribution of electrode beta values. To determine if the distribution of electrode beta values differed from zero, we computed, at each frequency, a *t*-test comparing the distribution to an expected mean of zero. To correct for multiple comparisons across our 240 statistical tests, we adjusted our significance threshold using a false discovery rate procedure with *q* set to 0.05. Only *p*-values less than our adjusted threshold of 0.0187 where deemed significant.

To capture the relationship of peak oscillatory frequency to the experimental/behavioral variables we performed a similar regression as above, replacing power at each frequency with the peak oscillatory frequency, such that:

$$\text{PeakFrequency}_{(e)} = \beta_{0(e)} + \beta_{1(e)}^{\text{Speed}} + \beta_{2(e)}^{\text{Mem}} + \beta_{3(e)}^{\text{Auto}} + \beta_{4(e)}^{\text{tNum}} + \epsilon \quad (4.2)$$

#### 4.4 Results

Of the nine patients, seven had electrodes localized to the hippocampus, for a total of 39 hippocampal electrodes. In addition to the hippocampus, the entire dataset contains 81 electrodes within the medial temporal lobe (inclusive of the hippocampus), 297 frontal lobe electrodes, 74 parietal lobe electrodes, 449 temporal lobe electrodes, and 61 occipital lobe electrodes. Only the 39 hippocampal electrodes are analyzed in this manuscript. Figure 4.2A shows the placement of one of the hippocampal electrodes from Patient 7, localized using our high resolution imaging techniques to hippocampal subfield CA1. On average, subjects pressed the button to indicate an objects' location within 9.55 ( $\pm 4.21$  s.d.) VR-units of the correct location (13.6% of total track length), indicating the subjects were able to reliably learn object locations by carefully attending to the location in the environment.

A key aim of our experimental design was to more reliably elicit low frequency oscillations in human hippocampus than have been seen in previous human virtual navigation studies. Figure 4.2B

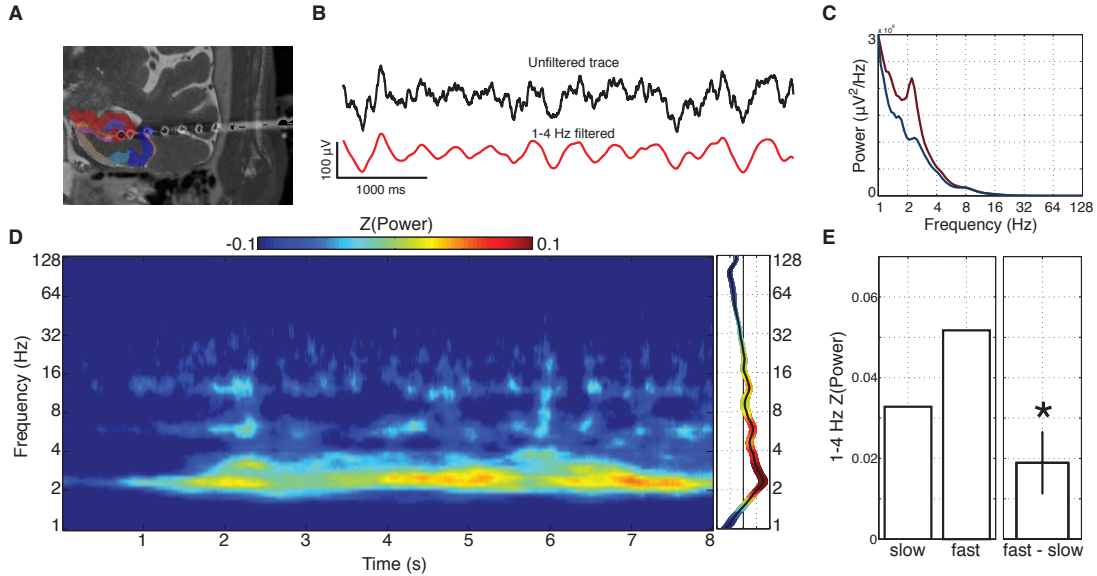


**Figure 4.2: Low frequency increases during virtual movement.** **A.** MRI of electrode localization for a depth probe in patient 7's hippocampus. MTL regions are shaded based on anatomical segmentation: red = CA1, pink = subiculum, purple = dentate gyrus, tan = entorhinal cortex, light blue = perirhinal cortex (BA35), dark blue = perirhinal cortex. The electrode indicated by the black circle is located in CA1. **B.** Unfiltered (black line) and filtered between 1 and 4 Hz (red line) voltage trace during a single movement trial, for the same electrode as in *A*. **C.** Power spectrum of all movement trials (red line) and baseline (blue line) for the same electrode during recording session 1. **D.** Time by frequency spectrogram for the first 8 seconds (left) and averaged across the trial durations (right) for all movement trials, averaged across all hippocampal electrodes in the dataset. The width of the shaded error region is  $\pm 1$  SEM, color coded to match the time x frequency spectrogram. **E.** Average Z-scored power between 1 and 4 Hz shown separately for fast and slow trials (left) and average increase in power for fast compared to slow trials. Error bar is  $\pm 1$  SEM ( $t(38) = 2.518$ ,  $p = 0.016$ , paired  $t$ -test).

shows a raw (top) and 1–4 Hz filtered (bottom) voltage trace from one movement trial of the task taken from the same electrode shown in Figure 4.2A, exhibiting a prominent  $\sim 2.5$  Hz oscillation. Figure 4.2C shows the electrode's power spectra for the same experimental session, averaged across all movement trials (red line), as well as the power spectra for the baseline period (blue line). There is a clear elevation in low frequencies and a distinct  $\sim 2.5$  Hz peak. We next quantified whether this pattern was reliable across the electrodes in our dataset.

We found that power of low frequencies of between approximately 2–4 Hz were the most elevated during virtual movement relative to baseline. As seen in Figure 4.2D, the time-frequency spectrogram averaged across all hippocampal electrodes in the dataset reveals a clear elevation in z-scored power at these low frequencies during movement periods. Also shown is the power spectrum averaged

across the entire duration of each trial, indicating that increased low frequency power is sustained for the duration of the movement period.

Having successfully elicited a general increase in low frequency power during periods of virtual movement, we next sought to determine whether the widely noted positive relationship between movement speed and rodent hippocampal theta power and frequency was also found in human hippocampus. We tested for a similar relationship in our data by comparing the average power of faster trials (upper 50% of trial-average speeds) and the slower trials (bottom 50%). As shown in Figure 4.2E, faster movement elicited significantly greater low frequency (1–4 Hz) power than slower movement ( $t(38) = 2.518, p = 0.016$ , paired  $t$ -test). Performing the same test at the traditional theta band of 4–8 Hz did not result in a significant difference between the movement speed conditions ( $p > 0.4$ ).

This increase in 1–4 Hz oscillatory power for faster compared to slower movements reveals that, as in the rodent, movement speed can strongly modulate hippocampal activity. However, given the complex role of theta activity in many aspects of cognition, we more fully characterized the explanatory power of multiple task variables, including speed, using a multivariate linear model. This approach, which researchers often employ to tease apart the relative contributions of task and behavioral factors to the overall spectral signal [Jacobs et al., 2006, Montgomery et al., 2009], was used here to quantify the relationship of movement speed, response accuracy, trial number, and automatic/manual movement to oscillatory power across a wide range of frequencies.

We observed a reliable positive relationship between trial-average movement speed and trial-average power at 1.8–2.5 Hz. Figure 4.3A shows the average  $\beta^{Speed}$  regression coefficient as a function of frequency, with significantly elevated beta values in frequencies between 1.8 and 2.4 Hz. This relationship is visible in individual univariate examples as well. Figures 4.3B and C plot average log-transformed power between 1.8 and 2.4 Hz as a function of movement speed for two example sessions with a strong linear relationship between power and speed, visible even when not statistically factoring out the effects of the other task variables. In total, 8 of 39 (20.5%) electrodes exhibited at least one session with a strong ( $p < .05$ ) positive univariate relationship between 1.8–

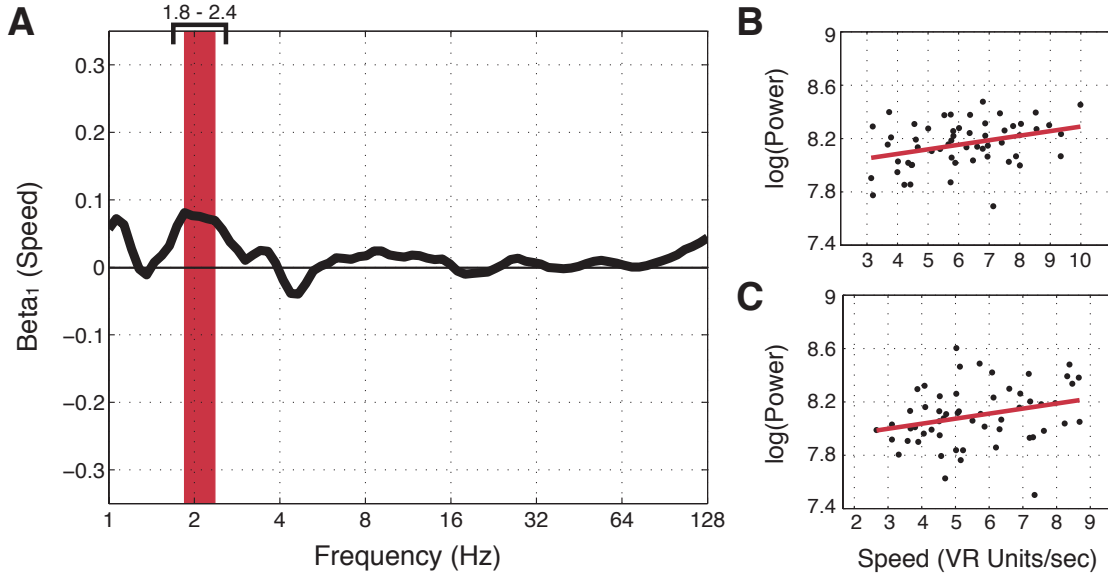


**Figure 4.3: Relationship of power and movement speed.** **A.** Regression coefficient for the speed predictor as a function of frequency, averaged across electrodes. The distribution of beta values was significant greater than zero between 1.8 and 2.4 Hz, indicating a positive relationship between power at that frequency range and movement speed ( $p$ 's less than the FDR corrected significance threshold of 0.0187). **B.** Average log transformed power between 1.8 and 2.4 Hz as a function of movement speed for a single session from an electrode from patient 5. **C.** Average log transformed power between 1.8 and 2.4 Hz as a function of movement speed for a single session from an electrode from patient 1.

2.4 Hz power and movement speed, compared to only 1 electrode that showed a negative effect. Of note, unlike oscillatory power, we did not find a corresponding relationship between peak oscillatory frequency any predictor variables, including speed.

Beyond modulations by movement, memory performance has been shown to strongly linked to human hippocampal oscillatory activity. Here, we observed reliable effects of memory performance on oscillatory power at a range of frequencies. Across all electrodes, the distribution of  $\beta^{Mem}$  values was significantly elevated at very low frequencies, such that increased power was associated with better memory performance. At frequencies between 5.9 and 14.9 Hz, the opposite was true, and increased power was associated with worse memory performance (see Figure 4.4A). In order to more fully understand this multifaceted relationship between power and performance in the task, we separately calculated the percent of electrodes that showed either a positive or negative relationship between memory performance and power at each frequency. As shown in Figure 4.4B, the frequency

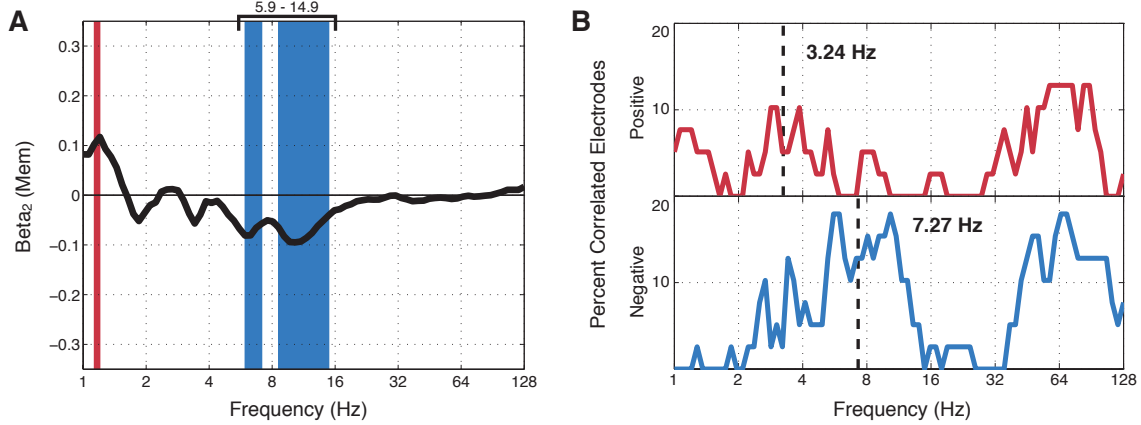


**Figure 4.4: Relationship of power and memory accuracy.** **A.** Regression coefficient for the memory accuracy predictor as a function of frequency, averaged across electrodes. The distribution of beta values was significant greater than zero for most of the range between 5.9 and 14.9 Hz, indicating a negative relationship between power at that frequency range and accuracy in the task, such that increased power is associated with worse performance ( $p$ 's less than the FDR corrected significance threshold of 0.0187). **B.** The percent of electrodes that showed a strong (regression  $p$ -value  $< .05$ ) relationship between memory performance and power at each frequency, separately for positive (top, red line) and negative (bottom, blue line) relationships.

range where the negative relationship was most prominent differed from the range where the positive relationship was greatest. Considering only frequencies below 32 Hz, the average center of mass where the greatest percentage of electrodes showed a significant positive relationship between power and memory performance was 3.24 Hz. For electrodes showing the opposite effect, the peak frequency was higher at 7.27 Hz.

Finally, we examined whether the spectral characteristics differed when patients were moved automatically through the environment as compared to when they moved themselves by actively pressing a button. Here, we found that active movement elicited greater power at a very wide range of frequencies, particularly between  $\sim 2$  and  $\sim 12$  Hz, and then again at frequencies above 48 Hz (see Figure 4.5A). As shown in Figure 4.5B, this broadband shift in the power spectrum is robust at the univariate level, with reliable differences between the conditions that closely mirrors the multivariate statistic. We also found that trial number was significantly positively related to oscillatory power at all frequencies below  $\sim 16$  Hz.

A unique feature of our task is that we can investigate not only the relationship between move-

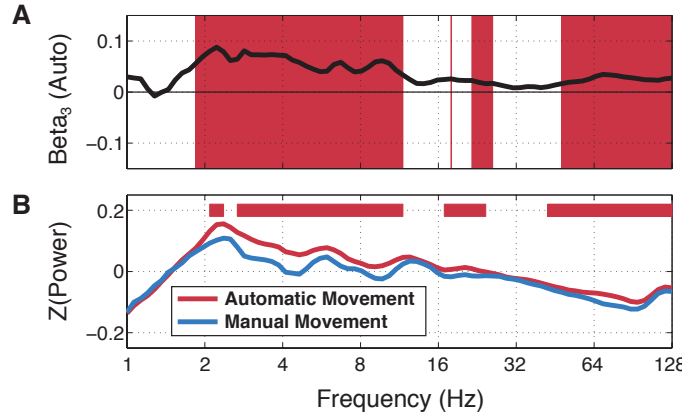


**Figure 4.5: Relationship of power and automatic/manual movement condition.** **A.** Regression coefficient for the automatic vs manual movement predictor as a function of frequency, averaged across electrodes. The distribution of beta values was significant greater than zero between 1.8 and 11.6 Hz, as well as at in the high gamma range, indicating a negative relationship between power at those frequencies range and automatic movement ( $p$ 's less than the FDR corrected significance threshold of 0.0187). **B.** The average z-scored power spectrum averaged across automatic movement trials (red line) and manual movement trials (blue line), with the difference between between the conditions plotted below and regions of significant differences shaded in red ( $t$ -tests;  $p$ 's less than FDR corrected significance threshold of 0.0318).

ment speed and neural activity, but also the effect of speed changes. On automatic movement trials, movement speed within each third of the track is chosen randomly between 2 VR-units/s and 12 VR-units/s. There is a 1 second ramp between each region, affording us a wide range of acceleration and deceleration values (this includes the beginning of the trial, where the initial speed is zero). Figure 4.6A shows the average time by frequency spectrogram aligned to the moment that a speed change begins and normalized to the preceding 250 ms. We find that there is general decrease in power, largely present across the entire range of frequencies. Also plotted is the average Z-scored power in the 1–4 Hz range, chosen because of the speed-related effects we previously discussed. Here, power begins to decrease near 750 ms following the onset of a speed change. When we separately examine accelerations and decelerations, it becomes clear that this negative effect is largely driven by increases in speed. Figure 4.6B shows the average power in the 2000 ms window following a speed change, where power is significantly decreased only for accelerations, and not significantly different from baseline for decelerations. Moreover, this effect is largest for higher magnitude accelerations.

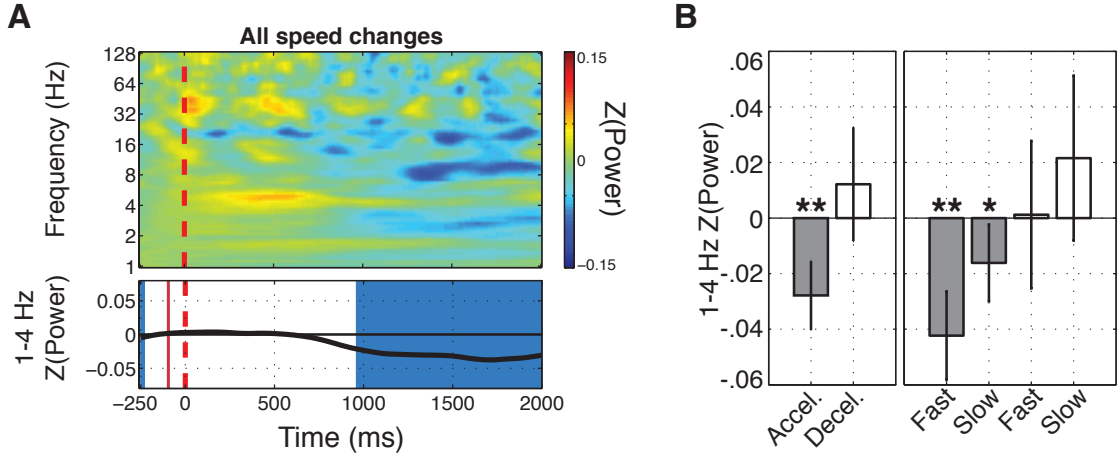


**Figure 4.6: Power modulation following changes in speed.** **A.** Time by frequency spectrograms beginning 250 ms before a speed change (top) and average 1–4 Hz z-scored power (bottom) over the same interval for all speed changes. Power is normalized relative the pre-speed change interval. Shaded blue regions indicate significant timepoints of decreased power (FDR corrected significant threshold of 0.0044). **B.** 1–4 Hz power averaged over the 0–2000 ms interval for all accelerations and all decelerations. Error bars are 95% confidence intervals ( $t$ -tests; \* =  $p < .05$ , \*\* =  $p < 10^{-4}$ .)

## 4.5 Discussion

The primary goal of the current study was to precisely characterize the relationship between hippocampal oscillatory activity and movement in a task where speed was explicitly manipulated. We first replicated the previous finding that low frequency power is increased during periods of virtual movement [Ekstrom et al., 2005]. We found that low frequency activity near 2 Hz was most strongly correlated with movement speed in the virtual environment. Though the 1–4 Hz range is commonly described as “delta”, our finding, along with other converging evidence, suggests that the functional equivalent of hippocampal theta activity actually occurs at lower frequencies in humans than in rodents (for reviews, see [Ekstrom and Watrous, 2014, Jacobs, 2014]). This raises the possibility that part of the explanation as to why human hippocampal “theta” has been difficult to find is that researchers have not been focusing on the most relevant frequencies. The approach taken in this study did not limit our analyses to predefined frequency bands, but rather searched for effects across a broad range of frequencies.

Across the population of electrodes, we found that 20.5% showed a strong single-session positive

univariate relationship between movement speed and low (1.8–2.4 Hz) frequency theta power. In contrast, the relationship between speed of movement and theta power is much more robust in rodents, such that the effect is visible in nearly all recordings taken from dorsal hippocampus, where spatial coding is the strongest [Hinman et al., 2011]. It is tempting to ascribe this difference to the fact that human studies rely upon virtual reality (VR) and lack the vestibular input of real world navigation, however recent studies examining rodent navigation in VR have found basic movement-related hippocampal properties to be generally conserved. Optic flow alone has been shown to be sufficient to elicit place cell responses [Harvey et al., 2009] and induce theta rhythmicity, though at a somewhat reduced amplitude [Chen et al., 2013]. Moreover, the positive relationship between speed and theta power is present in rodent VR, yet the relationship between speed and theta frequency is not [Ravassard et al., 2013], consistent with the results of the current study. As such, the interspecies distinction in the strength of the effect is most likely not due to the use of VR methods. One possibility that cannot at present be ruled out is the fact that most of our electrodes are placed in anterior hippocampus, which is thought to be analogous to rodent ventral hippocampus, where spatial coding is less precise and speed/theta effects are weakest [Kjelstrup et al., 2008, Long et al., 2015, Strange et al., 2014]. An important avenue of future work is to investigate whether this same functional delineation is present in the human hippocampus.

Our relatively low percentage speed-modulated electrodes is in line with a previous study showing theta power modulations as a function of speed [Watrous et al., 2011] in human hippocampus, where variables other than speed were more strongly associated with changes in oscillatory power. We found that low frequency power was strongly related to memory accuracy in the task. In our task, every traversal down the linear track also served as a test of memory, where memory accuracy was measured as the distance between a hidden objects' true location and the location where the participant thought it was located (as indicated via a button press). Thus, we represent memory with a continuous variable, unlike many studies where human memory is analyzed in a binary fashion (ie., an item is recalled or not recalled, or recognized or not recognized), allowing for a more fine grained measure of memory. We found that decreases in power between approximately 6 and 15 Hz were

associated with better memory performance, in what would be traditionally described as the theta and alpha bands. This result is consistent with a number of studies showing low frequency decreases correlate with successful memory encoding in the hippocampus [Burke et al., 2013, Hanslmayr and Staudigl, 2013, Long et al., 2014b, Sederberg et al., 2007].

The finding that decreases in theta power are linked to better memory is seemingly at odds with the notion, largely derived from rodent work, that theta is necessary for proper memory function. Work to reconcile these views has revealed the existence of two distinct “thetas”, a “slow theta” at ~3 Hz and a “fast theta” at ~8 Hz [Lega et al., 2012]. In this study by Lega et al. (2012), successful memory in a free recall task was associated with increases in slow theta and decreases in fast theta in the human hippocampus. A more in depth analyses of the memory-related effects in our study show quite similar results. The large decrease in power associated with good memory, centered at ~7 Hz, actually masked a lower frequency effect of increased power associated with good memory, centered at ~3 Hz. The heterogeneity of these effects suggests that the previous studies demonstrating low frequency decreases coinciding with successful memory may be overlooking such a “slow theta” effect when averaging the data across electrodes.

A final aspect of our studies concerns the effects of acceleration and automatic vs manually controlled movement on the overall spectral signal. We found that automatic movement elicited greater power than manually controlled movement across the majority of the examined power spectrum (Figure 4.5). This broadband upward shift in the power spectrum is somewhat surprising, given that self-motion induces greater theta power than forced movement in the rodent [Terrazas et al., 2005]. In addition, we found that periods of acceleration resulted in a general decrease in power. In the low theta range where movement speed and power were positively correlated, we found that faster accelerations led to a larger decrease in power as compared to slower accelerations and decelerations. This is fairly consistent with rodent findings that demonstrate that large abrupt changes in speed result in decreased theta power [Long et al., 2014a].

In rodents, a distinction is made between Type 1 and Type 2 theta. Type 1 (atropine-resistant) theta is more prominent during locomotion and centered around 7–8 Hz [Kramis et al., 1975],

and Type 2 theta occurs more frequently during immobility, is associated with arousal and fear conditioning, and exists at lower frequencies [Sainsbury et al., 1987, Seidenbecher et al., 2003]. Our findings of reliable relationships between power at frequencies below 4 Hz and both movement and memory function suggests that the functional analogue of rodent Type 1 theta truly exists in the canonical “delta” band, and that the standard frequency band naming conventions may, in this case, be obfuscating interspecies commonalities.

## Chapter 5: General discussion

### 5.1 Summary

In this dissertation, I recorded intracranial brain activity as patients traveled through carefully designed 3D virtual environments in order to investigate the neural signals related to spatial navigation and memory function. My work shows that the neural mechanisms responsible for representing external space are also involved in the storage and retrieval of episodic memories, helping to reconcile how the hippocampus and medial temporal lobe (MTL) can simultaneously be vital for both navigation and declarative memory abilities. I have also advanced our understanding of exactly how space is coded in the human brain using both single unit and oscillatory analyses, and I provide insights into how this neural system aligns with or differs from that in the more well characterized rodent brain.

In Chapter 2, I isolated place cells in the human MTL and examined whether their functional role extends beyond simply supporting a representation of space. Place cells have been identified in humans in only a small number of previous studies [Ekstrom et al., 2003, Jacobs et al., 2010a], thus the identification of place cells was a crucial first step in my analysis. We found that ~25% of MTL neurons had well defined place fields, such that they exhibited significantly elevated rates of spiking within the field compared to other areas of the virtual environment. Based upon models of human episodic memory function, we hypothesized that these place cells would not only be involved in coding for space, but should also reactivate when patients recalled events that occurred within the virtual environment. This hypothesis is grounded in a theoretical account of human memory known as *retrieved context*, which argues that when a memory is stored, it is stored along with its associated context. Here, context refers to an amalgam of both internal and external information present when an event occurs [Bower, 1972, McGeoch, 1942], including, but not limited to, space and time (hence, the term spatiotemporal context). When a memory is later recalled, the theory posits that the context is recovered as well [Howard and Kahana, 2002, Lohnas and Kahana, 2014, Polyn

et al., 2009b]. If place cells represent not just an internal map, but, moreover, the *spatial context* of a memory, then the pattern of place cell activity that represents a particular location should reemerge when events that occurred at that location are later recalled, even when the participant is no longer navigating the environment. Indeed, this is precisely what we find, such that place cell activity prior to and during the vocalization of a memory closely resembles place cell activity that codes for the location where the memory was formed.

The work described in Chapter 2 capitalized on the knowledge that place cells exist in human MTL and exhibit similar behavior to place cells found in rodents. However, our understanding of the intricacies of the neural representation of space in the human brain still lags far behind that of rodents, where numerous types of spatially tuned cells have been found and the distinctive functions of MTL subregions have been fairly well characterized (for a review of the rodent literature, see [Moser et al., 2008]). In Chapter 3, I attempted to partially close this gap by identifying additional classes of specialized cells beyond place cells in humans, as well as by highlighting key differences in the type of information coded by distinct MTL subregions. We first isolated cells in the MTL whose firing rates varied as a function of location within the virtual environment, and then we further sorted these cells based on the precise characteristics of their firing patterns. We found that cells predominantly located in the entorhinal cortex (EC) coded for multiple related locations in the virtual environment, in contrast to the standard place cell that fires at a single location. More specifically, these EC cells exhibited multiple firing fields such that individual cells spiked at the same relative location across multiple distinct regions of the environment, seemingly coding a measure of relative distance that is tied to environmental geometry. We labeled these cells *path equivalent* cells, as their properties are very similar to path equivalent cells previously found in rodent EC [Frank et al., 2000]. This finding nicely parallels the rodent literature, where there exists a diversity of cell classes in the EC that code for numerous environmental features [Derdikman et al., 2009, Fyhn et al., 2004, Hafting et al., 2005, Sargolini et al., 2006, Solstad et al., 2008].

In Chapter 4, I continued my comparison between rodent and human data, moving from analyses of neuronal spiking to analyses of oscillatory activity. Focusing solely on the hippocampus, I investi-

gated whether the *theta* oscillation, which plays so prominent a role in rodent spatial navigation, was similarly modulated by movement during human navigation. Though previous human studies have shown a general increase in low frequency hippocampal activity during periods of virtual movement [Caplan et al., 2003, Ekstrom et al., 2005, Jacobs et al., 2010b], my task was explicitly designed to test for the effects movement speed on neural activity, which is tightly coupled to theta power in the rodent [Vanderwolf, 1969]. I found that movement related oscillatory activity in the human hippocampus is consistently expressed at frequencies between 2 and 4 Hz, unlike the functionally analogous rodent signal which appears at ~7–8 Hz [Buzsáki, 2002]. Moreover, I showed that the amplitude of the theta signal increases as a function of movement speed, replicating the longstanding rodent phenomenon [McFarland et al., 1975]. In addition to movement related oscillatory activity, I also examined the relationship between low frequency activity and memory for object locations within the virtual environment. I found that a “slow theta” signal present at ~3 Hz was correlated with better memory performance whereas a “fast theta” at ~7 Hz was correlated with worse memory performance, building on previous work showing that grouping signals into their traditional frequency bands may mask underlying effects [Lega et al., 2012].

## 5.2 Regional differences in medial temporal lobe spatial coding

What are the distinctive roles of various MTL subregions, in particular, the hippocampus and the entorhinal cortex, in coding for space? As mentioned in Chapter 2 and highlighted in Chapter 3, there are many different types of spatially tuned cells. Hippocampal place cells create a seemingly allocentric (map based) representation of external space [Muller, 1996, O’Keefe and Dostrovsky, 1971]. This representation is formed based upon features of the environment, such as salient landmarks [O’Keefe and Burgess, 1996]. Notably, when a rodent is moved between environments or aspects of the current environment are changed, the hippocampal spatial code undergoes a process known as *remapping* [Muller and Kubie, 1987]. When remapping occurs, a place cell that was active in one environment may not be active in another, or it may alter the location of its place field to represent a completely new area of space [Leutgeb et al., 2005a, 2004, Markus et al., 1995]. In contrast, cells in upstream brain regions, like the EC, tend to provide a quite different sort of information, such

that they do not code for precise locations in specific environments. Rather, the activity of these cells is largely invariant to the specific environmental features. Grid cells that are co-active in one environment are likely to be co-active in another and will maintain the spacing of their firing locations [Fyhn et al., 2007]. Similarly, the population activity of head direction cells is coherent across environments [Taube et al., 1990], and, likewise, a border cell that fires along the west wall of one environment will continue to fire along the west wall of a new environment [Solstad et al., 2008]. Thus, these cells are believed to provide part of the neural metric for calculating location based on self-motion, or, in other words, the ability to perform path integration independent of particular environmental features [Buzsáki and Moser, 2013, Jeffery and Burgess, 2006].

My work discovering path equivalent cells in the human EC is one of the few attempts to quantify the functional differentiation between human MTL regions at the level of single neurons, though the literature is beginning to grow. In addition to place cells in hippocampus [Ekstrom et al., 2003], “path cells” have been found in human EC that code for circular direction of travel [Jacobs et al., 2010a], and human analogues of EC grid cells have recently be located as well [Jacobs et al., 2013]. The method through which non-specific EC signals are transformed into the precise firing of hippocampal cells is a current topic of great interest. Given that many EC neurons synapse directly onto hippocampal place cells [Zhang et al., 2013], it is believed the the location specificity of place cells in the hippocampus is facilitated in part by the transmission of a diverse array of EC input [Moser and Moser, 2013]. This hypothesis is compatible with my findings, though the exact mechanisms of such a transformation are not yet understood.

### 5.3 Beyond space in the hippocampus

In the rodent literature, there has been a longstanding debate about the exact nature of the hippocampus. Namely, does the hippocampus act, fundamentally, as cognitive map that encodes the surrounding spatial features, or has the fact that many hippocampal cells are so strongly tuned to space caused researchers to overlook non-spatial coding properties of the hippocampus [Eichenbaum et al., 1999]? The cognitive mapping hypothesis, popularized by O’Keefe and Nadel [1978] held great sway in the field for a number of decades, but more recent work has begun to reveal that cells in the

rodent hippocampus are modulated by many variables beyond spatial information. Hippocampal cells have been shown to respond to non-spatial factors such as texture, odor, and color [Igarashi et al., 2014, Leutgeb et al., 2005a, Wood et al., 1999, Young et al., 1994]. Moreover, the firing patterns of place cells are affected by task demands, such that they distinguish between future goal locations [Ferbinteanu and Shapiro, 2003, Wood et al., 2000], conjunctively code for item and place information [Komorowski et al., 2009], and can keep track of temporal order [Manns et al., 2007]. Intriguingly, newly discovered hippocampal *time cells* provide a mechanism for self-localizing in time in addition to self-localizing in space [Kraus et al., 2013, MacDonald et al., 2011]. These findings point towards a broader role of hippocampal function in the rodent beyond providing a pure map of space and into the realm of memory function.

The work I described in Chapter 2 builds off this line of thinking by investigating how the pre-supposed spatial representation system of the hippocampus interfaces with human episodic memory abilities. By showing that place cells are a neural mechanism allowing for memory episodes to become “tagged” with the location where they occurred, I revealed a concrete link between the spatial coding properties of the hippocampal formation and episodic memory function. This integration further strengthens the hypothesis that hippocampal activity can be conceptualized not just in terms of its relation to external space, but rather as part of a general engine of episodic memory, of which space is a core component.

#### **5.4 From rodents to humans**

At its core, a major aim of my work is to test theories of MTL function that are derived from rodent data with neural activity recorded directly from humans. As I’ve outlined, there are certainly many interspecies commonalities, such as the place cells I’ve shown in Chapter 2, the EC path equivalent cells I discussed in Chapter 3, and the presence of movement related oscillatory activity highlighted in Chapter 4. However, in spite of these similarities, key differences have emerged. In particular, hippocampal movement related oscillations appear at different frequencies in the rodent and in humans. In humans, this signal seems to exist between 2 and 4 Hz, much slower than the traditional theta signal in rodents. My findings are consistent with converging results indicating that human

hippocampal theta is present at lower frequencies than in rodents [Jacobs, 2014, Watrous et al., 2013], and raises concerns about the applicability of rodent-derived models of brain function that rely the precise frequency of the theta oscillation [Burgess et al., 2007, Jensen and Lisman, 1998].

## 5.5 Future directions and concluding remarks

Throughout this dissertation, the historical distinction between the spatial coding properties of the medial temporal lobe studied primarily in rodents and the memory-centric properties studied primarily in humans has framed much of my work. How do animals maintain a neural representation of their environment? How do humans encode and retrieve new memories? Given that these two phenomena make use of the same neural structures, are they actually distinct systems, or are we simply viewing the same system through two different lenses? This idea that the navigation “system” and the memory “system” are, in fact, part of a largely unitary construct is not new, but it is only recently that precise explanatory theories have been put forth. In one view, the neural representation of space in the rodent is an evolutionary precursor to declarative memory abilities in humans [Buzsáki and Moser, 2013]. Here, the ability to store and retrieve memories relies on the same neural computations responsible for keeping track of location in space. In another view, the hippocampus is thought of not in spatial terms or in memory terms, but rather as being the seat of relational processing [Cohen and Eichenbaum, 1993, Eichenbaum, 2014]. The discovery that many hippocampal cells keep track of time in addition to location [MacDonald et al., 2011, Pastalkova et al., 2008] provides the neural circuitry necessary to bind co-occurring events together in both time and space.

Regardless of the precise mechanism, I believe my work serves to further this view that the neural representations of space and the neural mechanisms underlying memory function are not as distinct from one another as previously thought. The ability to study direct neural activity from humans allows to us to build upon the important work done in the rodent domain, and it also, importantly, allows us to test spatial navigation and memory function simultaneously in ways that are not possible in rodent research. There is, of course, still much that remains unanswered. In the final section, I briefly highlight some areas of potential future investigation.

**Intra-hippocampal distinctions in spatial coding** Research investigating the spatial coding properties of the human hippocampus, has, thus far, treated the hippocampus as a single structure, implicitly assuming that the hippocampus is uniform in its function. This is, unsurprisingly, not entirely true. Anatomically, the hippocampus can be broken down into a number of subfields, in particular CA1, CA3, and dentate gyrus [Andersen et al., 2006]. Rodent work has shown that, while all of these regions contain spatially selective cells, they are dissociable in their behaviors, specifically with regards to place cell remapping [Leutgeb et al., 2007, 2005b, Leuthardt et al., 2004]. In addition to this architectural delineation, the hippocampus exhibits a functional gradient along its longitudinal axis, such that the rodent dorsal hippocampus is associated with more precise spatial turning and the ventral hippocampus is associated with a coarser representation of space [Kjelstrup et al., 2008, Strange et al., 2014].

The reason for the oversimplification of hippocampal anatomy in humans is largely technical – it has been difficult to tell exactly where in the hippocampus electrodes are placed. However, recent work combining advanced computational algorithms and higher resolution MRI techniques has made precise electrode localizations possible [Dykstra et al., 2012, Yushkevich et al., 2015]. Going forward, mapping human hippocampus with the same level of anatomical detail as done in the rodent will be a valuable step in our understanding of hippocampal function.

**The role of theta phase in spatial coding, memory, and neuronal communication** My work has focused on the amplitude of oscillatory activity, but the phase of the signal provides an additional source of information. Specifically, the phase of the theta oscillation has been shown to be tightly coupled to many aspects of neural computation and communication. In many ways, theta is thought to be a timing signal that coordinates the activity of assemblies of neurons [Buzsáki, 2005]. Place cell activity is tied to the phase of the ongoing theta rhythm in rodents [O’Keefe and Recce, 1993, Skaggs et al., 1996], and the phase of the theta oscillation contains complementary information about a rodent’s location in the environment [Agarwal et al., 2014]. Beyond spatial coding, the phase of an oscillation is related to synaptic plasticity [Buzsáki and Draguhn, 2004, Huerta and Lisman, 1993] and, through the phenomenon known as phase-amplitude coupling (where the phase of theta is

coupled to the amplitude of a higher frequency oscillation), involved in inter-region communication [Colgin et al., 2009].

In humans, the phase of oscillatory signals is beginning to receive more attention. The spiking activity of human hippocampal neurons is often “phase-locked” to low frequency oscillations [Jacobs et al., 2007], which is predictive of successful memory formation [Rutishauser et al., 2010]. Phase-amplitude coupling has also been shown to correlate with successful memory formation [Canolty et al., 2006, Lega et al., In press]. The role of phase and its relationship to the neural representation of space, however, has not yet been directly studied in humans. Thus, aligning phase analyses across rodent and human data represents a relatively new and promising avenue of research

## Bibliography

- Agarwal, G., Stevenson, I. H., Berényi, A., Mizuseki, K., Buzsáki, G., and Sommer, F. T. Spatially distributed local fields in the hippocampus encode rat position. *Science*, 344(6184):626–630, 2014.
- Aghajan, Z. M., Acharya, L., Moore, J. J., Cushman, J. D., Vuong, C., and Mehta, M. R. Impaired spatial selectivity and intact phase precession in two-dimensional virtual reality. *Nature neuroscience*, 2014.
- Allen, K., Rawlins, J. N. P., Bannerman, D. M., and Csicsvari, J. Hippocampal place cells can encode multiple trial-dependent features through rate remapping. *The Journal of Neuroscience*, 32(42):14752–14766, 2012.
- Andersen, P., Morris, R., Amaral, D., Bliss, T., and O’Keefe, J. *The hippocampus book*. Oxford University Press, 2006.
- Benjamini, Y. and Hochberg, Y. Controlling the False Discovery Rate: a practical and powerful approach to multiple testing. *Journal of Royal Statistical Society, Series B*, 57:289–300, 1995.
- Bird, C. and Burgess, N. The hippocampus and memory: insights from spatial processing. *Nature Reviews Neuroscience*, 9(3):182–194, 2008.
- Bjerknes, T. L., Moser, E. I., and Moser, M.-B. Representation of geometric borders in the developing rat. *Neuron*, 82(1):71–78, 2014.
- Bower, G. H. Stimulus-sampling theory of encoding variability. In Melton, A. W. and Martin, E., editors, *Coding Processes in Human Memory*, chapter 5, pages 85–121. John Wiley and Sons, New York, 1972.
- Brun, V., Solstad, T., Kjelstrup, K., Fyhn, M., Witter, M., Moser, E., and Moser, M. Progressive increase in grid scale from dorsal to ventral medial entorhinal cortex. *Hippocampus*, 18(12):1200–1212, 2008.
- Buckmaster, C., Eichenbaum, H., Amaral, D., Suzuki, W., and Rapp, P. Entorhinal Cortex Lesions Disrupt the Relational Organization of Memory in Monkeys. *Journal of Neuroscience*, 24(44):9811–9825, 2004.
- Burgess, N., Barry, C., O’Keefe, J., and London, U. An oscillatory interference model of grid cell firing. *Hippocampus*, 17(9):801–12, 2007.
- Burke, J. F., Zaghloul, K. A., Jacobs, J., Williams, R. B., Sperling, M. R., Sharan, A. D., and Kahana, M. J. Synchronous and asynchronous theta and gamma activity during episodic memory formation. *Journal of Neuroscience*, 33(1):292–304, 2013.
- Buzsáki, G. Theta oscillations in the hippocampus. *Neuron*, 33(3):325–340, 2002.
- Buzsáki, G. Theta rhythm of navigation: Link between path integration and landmark navigation, episodic and semantic memory. *Hippocampus*, 15:827–840, 2005.
- Buzsáki, G. and Moser, E. Memory, navigation and theta rhythm in the hippocampal-entorhinal system. *Nature Neuroscience*, 16(2):130–138, 2013.
- Buzsáki, G. and Draguhn, A. Neuronal oscillations in cortical networks. *Science*, 304(5679):1926–1929, 2004. doi: 10.1126/science.1099745.

- Canolty, R. T., Edwards, E., Dalal, S. S., Soltani, M., Nagarajan, S. S., Kirsch, H. E., Berger, M. S., Barbaro, N. M., and Knight, R. T. High gamma power is phase-locked to theta oscillations in human neocortex. *Science*, 313(5793):1626–1628, 2006.
- Caplan, J. B., Madsen, J. R., Schulze-Bonhage, A., Aschenbrenner-Scheibe, R., Newman, E. L., and Kahana, M. J. Human theta oscillations related to sensorimotor integration and spatial learning. *Journal of Neuroscience*, 23:4726–4736, 2003.
- Chen, G., King, J. A., Burgess, N., and O’Keefe, J. How vision and movement combine in the hippocampal place code. *Proceedings of the National Academy of Sciences, USA*, 110(1):378–383, 2013.
- Clayton, N., Bussey, T., and Dickinson, A. Can animals recall the past and plan for the future? *Nature Reviews Neuroscience*, 4(8):685–691, 2003.
- Cohen, N. J. and Eichenbaum, H. *Memory, amnesia, and the hippocampal system*. MIT, Cambridge, MA, 1993.
- Colgin, L., Denninger, T., Fyhn, M., Hafting, T., Bonnevie, T., Jensen, O., Moser, M., and Moser, E. Frequency of gamma oscillations routes flow of information in the hippocampus. *Nature*, 462 (7271):353–357, 2009.
- Davachi, L. Item, context and relational episodic encoding in humans. *Current Opinion in Neurobiology*, 16(6):693—700, 2006.
- Davachi, L., Mitchell, J. P., and Wagner, A. D. Multiple routes to memory: distinct medial temporal lobe processes build item and source memories. *Proceedings of the National Academy of Sciences, USA*, 100(4):2157 – 2162, 2003.
- Derdikman, D., Whitlock, J., Tsao, A., Fyhn, M., Hafting, T., Moser, M., and Moser, E. Fragmentation of grid cell maps in a multicompartment environment. *Nature Neuroscience*, 12(10): 1325–1332, 2009.
- Dykstra, A. R., Chan, A. M., Quinn, B. T., Zepeda, R., Keller, C. J., Cormier, J., Madsen, J. R., Eskandar, E. N., and Cash, S. S. Individualized localization and cortical surface-based registration of intracranial electrodes. *Neuroimage*, 59(4):3563–3570, 2012.
- Eichenbaum, H., Dudchenko, P., Wood, E., Shapiro, M., and Tanila, H. The hippocampus, memory, and place cells: is it spatial memory or a memory space? *Neuron*, 23(2):209–226, 1999.
- Eichenbaum, H. Hippocampus: cognitive processes and neural representations that underlie declarative memory. *Neuron*, 44(1):109–120, Sep 2004. doi: 10.1016/j.neuron.2004.08.028. URL <http://dx.doi.org/10.1016/j.neuron.2004.08.028>.
- Eichenbaum, H. Time cells in the hippocampus: a new dimension for mapping memories. *Nature Reviews Neuroscience*, 15(11):732–744, 2014.
- Eichenbaum, H. and Lipton, P. A. Towards a functional organization of the medial temporal lobe memory system: role of the parahippocampal and medial entorhinal cortical areas. *Hippocampus*, 18(12):1314–1324, 2008.
- Ekstrom, A. D. and Watrous, A. J. Multifaceted roles for low-frequency oscillations in bottom-up and top-down processing during navigation and memory. *NeuroImage*, 85(2):667 – 677, 2014.
- Ekstrom, A. D., Kahana, M. J., Caplan, J. B., Fields, T. A., Isham, E. A., Newman, E. L., and Fried, I. Cellular networks underlying human spatial navigation. *Nature*, 425:184–187, 2003.
- Ekstrom, A. D., Caplan, J., Ho, E., Shattuck, K., Fried, I., and Kahana, M. Human hippocampal theta activity during virtual navigation. *Hippocampus*, 15:881–889, 2005.

- Ferbinteanu, J. and Shapiro, M. L. Prospective and retrospective memory coding in the hippocampus. *Neuron*, 40(6):1227–1239, 2003.
- Frank, L. M., Brown, E. N., and Wilson, M. Trajectory encoding in the hippocampus and entorhinal cortex. *Neuron*, 27(1):169–178, 2000.
- Fried, I., Wilson, C., Maidment, N., Engel, J. J., Behnke, E., Fields, T., MacDonald, K., Morrow, J., and Ackerson, L. Cerebral microdialysis combined with single-neuron and electroencephalographic recording in neurosurgical patients. *Journal of Neurosurgery*, 91:697–705, 1999.
- Fyhn, M., Molden, S., Witter, M., Moser, E., and Moser, M. Spatial representation in the entorhinal cortex. *Science*, 305:1258–1264, 2004.
- Fyhn, M., Hafting, T., Treves, A., Molden, S., Moser, M.-B., and Moser, E. I. Hippocampal remapping and grid realignment in entorhinal cortex. *Nature*, 446:190–194, 2007.
- Gelbard-Sagiv, H., Mukamel, R., Harel, M., Malach, R., and Fried, I. Internally generated reactivation of single neurons in human hippocampus during free recall. *Science*, 3:96–101, 2008.
- Guderian, S., Schott, B., Richardson-Klavehn, A., and Duzel, E. Medial temporal theta state before an event predicts episodic encoding success in humans. *Proceedings of the National Academy of Sciences, USA*, 106(13):5365, 2009.
- Hafting, T., Fyhn, M., Molden, S., Moser, M.-B., and Moser, E. I. Microstructure of a spatial map in the entorhinal cortex. *Nature*, 436:801–806, 2005. doi: 10.1038/nature03721.
- Hanslmayr, S. and Staudigl, T. How brain oscillations form memories—a processing based perspective on oscillatory subsequent memory effects. *NeuroImage*, 2013.
- Hargreaves, E., Rao, G., Lee, I., and Knierim, J. Major dissociation between medial and lateral entorhinal input to dorsal hippocampus. *Science*, 308(5729):1792–1794, 2005.
- Harvey, C., Collman, F., Dombeck, D., and Tank, D. Intracellular dynamics of hippocampal place cells during virtual navigation. *Nature*, 461:941–946, 2009.
- Hasselmo, M. E. *How We Remember: Brain Mechanisms of Episodic Memory*. MIT Press, Cambridge, MA, 2012.
- Hasselmo, M. E. and Stern, C. E. Theta rhythm and the encoding and retrieval of space and time. *Neuroimage*, 85:656–666, 2014.
- Hinman, J. R., Penley, S. C., Long, L. L., Escabí, M. A., and Chrobak, J. J. Septotemporal variation in dynamics of theta: speed and habituation. *Journal of neurophysiology*, 105(6):2675–2686, 2011.
- Howard, M. W. and Kahana, M. J. A distributed representation of temporal context. *Journal of Mathematical Psychology*, 46(3):269–299, 2002.
- Howard, M. W., Fotedar, M. S., Datey, A. V., and Hasselmo, M. E. The temporal context model in spatial navigation and relational learning: Toward a common explanation of medial temporal lobe function across domains. *Psychological Review*, 112(1):75–116, 2005.
- Howard, M. W., Viskontas, I. V., Shankar, K. H., and Fried, I. Ensembles of human MTL neurons “jump back in time” in response to a repeated stimulus. *Hippocampus*, 22:1833–1847, 2012. doi: 10.1002/hipo.22018.
- Huerta, P. T. and Lisman, J. E. Heightened synaptic plasticity of hippocampal CA1 neurons during a cholinergically induced rhythmic state. *Nature*, 364(6439):723–725, 1993.
- Igarashi, K. M., Lu, L., Colgin, L. L., Moser, M.-B., and Moser, E. I. Coordination of entorhinal-hippocampal ensemble activity during associative learning. *Nature*, 510(7503):143–147, 2014.

- Jacobs, J. and Kahana, M. J. Direct brain recordings fuel advances in cognitive electrophysiology. *Trends in Cognitive Sciences*, 14(4):162–171, 2010.
- Jacobs, J., Hwang, G., Curran, T., and Kahana, M. J. EEG oscillations and recognition memory: Theta correlates of memory retrieval and decision making. *NeuroImage*, 15(2):978–87, 2006.
- Jacobs, J., Kahana, M. J., Ekstrom, A. D., and Fried, I. Brain oscillations control timing of single-neuron activity in humans. *Journal of Neuroscience*, 27(14):3839–3844, 2007.
- Jacobs, J., Kahana, M. J., Ekstrom, A. D., Mollison, M. V., and Fried, I. A sense of direction in human entorhinal cortex. *Proceedings of the National Academy of Sciences*, 107(14):6487–6482, 2010a.
- Jacobs, J., Korolev, I., Caplan, J., Ekstrom, A., Litt, B., Baltuch, G., Fried, I., Schulze-Bonhage, A., Madsen, J., and Kahana, M. Right-lateralized brain oscillations in human spatial navigation. *Journal of Cognitive Neuroscience*, 22(5):824–836, 2010b.
- Jacobs, J., Weidemann, C. T., Miller, J. F., Solway, A., Burke, J. F., Wei, X., Suthana, N., Sperling, M. R., Sharan, A. D., Fried, I., and Kahana, M. J. Direct recordings of grid-like neuronal activity in human spatial navigation. *Nature Neuroscience*, 16:1188–1190, 2013.
- Jacobs, J. Hippocampal theta oscillations are slower in humans than in rodents: implications for models of spatial navigation and memory. *Philosophical Transactions of the Royal Society B: Biological Sciences*, 369(1635):20130304, 2014.
- Jeffery, K. J. and Burgess, N. A metric for the cognitive map: Found at last? *Trends in Cognitive Sciences*, 10:1–3, 2006.
- Jensen, O. and Lisman, J. E. An oscillatory short-term memory buffer model can account for data on the Sternberg task. *J. Neuroscience*, 18:10688–10699, 1998.
- Kahana, M. J., Sekuler, R., Caplan, J. B., Kirschen, M., and Madsen, J. R. Human theta oscillations exhibit task dependence during virtual maze navigation. *Nature*, 399:781–784, 1999.
- Kahana, M. J. The cognitive correlates of human brain oscillations. *Journal of Neuroscience*, 26(6): 1669–1672, 2006. doi: 10.1523/JNEUROSCI.3737-05c.2006.
- Khan, U. A., Liu, L., Provenzano, F. A., Berman, D. E., Profaci, C. P., Sloan, R., Mayeux, R., Duff, K. E., and Small, S. A. Molecular drivers and cortical spread of lateral entorhinal cortex dysfunction in preclinical alzheimer's disease. *Nature neuroscience*, 17(2):304–311, 2014.
- Kjelstrup, K., Solstad, T., Brun, V., Hafting, T., Leutgeb, S., Witter, M., Moser, E., and Moser, M. Finite scale of spatial representation in the hippocampus. *Science*, 321(5885):140–143, 2008.
- Klimesch, W., Doppelmayr, M., Russegger, H., and Pachinger, T. Theta band power in the human scalp EEG and the encoding of new information. *NeuroReport*, 7:1235–1240, 1996.
- Knierim, J., Lee, I., and Hargreaves, E. Hippocampal Place Cells: Parallel Input Streams, Subregional Processing, and Implications for Episodic Memory. *Hippocampus*, 16:755–764, 2006.
- Komorowski, R., Manns, J., and Eichenbaum, H. Robust conjunctive item-place coding by hippocampal neurons parallels learning what happens where. *Journal of Neuroscience*, 29(31):9918, 2009.
- Kramis, R., Vanderwolf, C., and Bland, B. Two types of hippocampal rhythmical slow activity in both the rabbit and the rat: relations to behavior and effects of atropine, diethyl ether, urethane, and pentobarbital. *Exp Neurol*, 49(1 Pt 1):58–85, 1975.
- Kraus, B. J., Robinson II, R. J., White, J. A., Eichenbaum, H., and Hasselmo, M. E. Hippocampal “time cells”: Time versus path integration. *Neuron*, 2013.

- Lachaux, J. P., Rudrauf, D., and Kahane, P. Intracranial EEG and human brain mapping. *Journal of Physiology-Paris*, 97(4–6):613–628, 2003.
- Lega, B. C., Burke, J. F., Jacobs, J., and Kahana, M. J. Slow theta-to-gamma phase amplitude coupling in human hippocampus supports the formation of new episodic memories. *Cerebral Cortex*, In press.
- Lega, B. C., Jacobs, J., and Kahana, M. Human hippocampal theta oscillations and the formation of episodic memories. *Hippocampus*, 22(4):748–761, 2012.
- Lenck-Santini, P.-P., Fenton, A. A., and Muller, R. U. Discharge properties of hippocampal neurons during performance of a jump avoidance task. *The Journal of Neuroscience*, 28(27):6773–6786, 2008.
- Leutgeb, J., Leutgeb, S., Moser, M., and Moser, E. Pattern Separation in the Dentate Gyrus and CA3 of the Hippocampus. *Science*, 315(5814):961, 2007.
- Leutgeb, S., Leutgeb, J., Moser, M., and Moser, E. Place cells, spatial maps and the population code for memory. *Current Opinion in Neurobiology*, 15:738–746, 2005a.
- Leutgeb, S., Leutgeb, J. K., Treves, A., Moser, M.-B., and Moser, E. I. Distinct ensemble codes in hippocampal areas ca3 and ca1. *Science*, 305(5688):1295–1298, 2004.
- Leutgeb, S., Leutgeb, J. K., Barnes, C. A., Moser, E. I., McNaughton, B. L., and Moser, M.-B. Independent codes for spatial and episodic memory in hippocampal neuronal ensembles. *Science*, 309(5734):619–623, 2005b.
- Leuthardt, E., Schalk, G., Wolpaw, J., Ojemann, J., and Moran, D. A brain-computer interface using electrocorticographic signals in humans. *Journal of Neural Engineering*, 1:63–71, 2004.
- Lohnas, L. J. and Kahana, M. J. A retrieved context account of spacing and repetition effects in free recall. *Journal of Experimental Psychology: Learning Memory and Cognition*, 40(3):755–764, 2014. doi: 10.1037/a0035585.
- Long, L. L., Hinman, J. R., Chen, C.-M., Escabi, M. A., and Chrobak, J. J. Theta dynamics in rat: speed and acceleration across the septotemporal axis. *PloS one*, 9(5):e97987, 2014a.
- Long, L. L., Bunce, J. G., and Chrobak, J. J. Theta variation and spatiotemporal scaling along the septotemporal axis of the hippocampus. *Frontiers in systems neuroscience*, 9, 2015.
- Long, N. M., Burke, J. F., and Kahana, M. J. Subsequent memory effect in intracranial and scalp eeg. *NeuroImage*, 84:488–494, 2014b.
- MacDonald, C., Lepage, K., Eden, U., and Eichenbaum, H. Hippocampal “time cells” bridge the gap in memory for discontiguous events. *Neuron*, 71(4):737–749, 2011.
- Manning, J. R., Polyn, S. M., Baltuch, G., Litt, B., and Kahana, M. J. Oscillatory patterns in temporal lobe reveal context reinstatement during memory search. *Proceedings of the National Academy of Sciences, USA*, 108(31):12893 – 12897, 2011.
- Manning, J. R., Sperling, M. R., Sharan, A., Rosenberg, E. A., and Kahana, M. J. Spontaneously reactivated patterns in frontal and temporal lobe predict semantic clustering during memory search. *Journal of Neuroscience*, 32(26):8871–8878, 2012.
- Manns, J. R., Howard, M. W., and Eichenbaum, H. Gradual changes in hippocampal activity support remembering the order of events. *Neuron*, 56(3):530–540, 2007. ISSN 0896-6273 (Print). doi: 10.1016/j.neuron.2007.08.017.
- Markus, E. J., Qin, Y. L., Leonard, B., Skaggs, W. E., McNaughton, B. L., and Barnes, C. A. Interactions between location and task affect the spatial and directional firing of hippocampal neurons. *Journal of Neuroscience*, 15(11):7079, 1995.

- Markus, E. J., Barnes, C. A., McNaughton, B. L., Gladden, V. L., and Skaggs, W. E. Spatial information content and reliability of hippocampal ca1 neurons: effects of visual input. *Hippocampus*, 4(4):410–421, 1994.
- McFarland, W. L., Teitelbaum, H., and Hedges, E. K. Relationship between hippocampal theta activity and running speed in the rat. *Journal of comparative and physiological psychology*, 88(1):324, 1975.
- McGeoch, J. A. *The psychology of human learning: An introduction*. Longmans, New York, 1942.
- McNaughton, B. L., Battaglia, F. P., Jensen, O., Moser, E. I., and Moser, M.-B. Path integration and the neural basis of the ‘cognitive map’. *Nature Reviews Neuroscience*, 7:663–678, 2006a. doi: 10.1038/nrn1932. URL <http://dx.doi.org/10.1038/nrn1932>.
- McNaughton, N., Ruan, M., and Woodnorth, M.-A. Restoring theta-like rhythmicity in rats restores initial learning in the morris water maze. *Hippocampus*, 16(12):1102–1110, 2006b.
- Miller, J. F., Lazarus, E., Polyn, S. M., and Kahana, M. J. Spatial clustering during memory search. *Journal of Experimental Psychology: Learning, Memory and Cognition*, 39(3):773–781, 2013.
- Miller, K. J., Leuthardt, E. C., Schalk, G., Rao, R. P. N., Anderson, N. R., Moran, D. W., Miller, J. W., and Ojemann, J. G. Spectral changes in cortical surface potentials during motor movement. *Journal of Neuroscience*, 27:2424–2432, 2007.
- Montgomery, S., Betancur, M., and Buzsaki, G. Behavior-dependent coordination of multiple theta dipoles in the hippocampus. *Journal of Neuroscience*, 29(5):1381, 2009.
- Mormann, F., Kornblith, S., Quiroga, R., Kraskov, A., Cerf, M., Fried, I., and Koch, C. Latency and selectivity of single neurons indicate hierarchical processing in the human medial temporal lobe. *Journal of Neuroscience*, 28(36):8865, 2008.
- Moser, E., Kropff, E., and Moser, M. Place cells, grid cells, and the brain’s spatial representation system. *Annu Rev Neurosci*, 31:69–89, 2008.
- Moser, E. and Moser, M. Grid cells and neural coding in high-end cortices. *Neuron*, 80:765–774, 2013.
- Muller, R. A quarter of a century of place cells. *Neuron*, 17:813–822, 1996.
- Muller, R., Bostock, E., Taube, J., and Kubie, J. On the directional firing properties of hippocampal place cells. *Journal of Neuroscience*, 14:7235, 1994.
- Muller, R. U. and Kubie, J. L. The effects of changes in the environment on the spatial firing of hippocampal complex-spike cells. *Journal of Neuroscience*, 7(7):1951–1968, 1987.
- Norman, K. A. and O’Reilly, R. C. Modeling hippocampal and neocortical contributions to recognition memory: A complementary learning systems approach. *Psychological Review*, 110:611–646, 2003.
- O’Keefe, J. and Burgess, N. Geometric determinants of the place fields of hippocampal neurons. *Nature*, 381(6581):425–428, 1996.
- O’Keefe, J. and Dostrovsky, J. The hippocampus as a spatial map: Preliminary evidence from unit activity in the freely-moving rat. *Brain Research*, 34:171–175, 1971.
- O’Keefe, J. and Nadel, L. *The hippocampus as a cognitive map*. Oxford University Press, New York, 1978.
- O’Keefe, J. and Recce, M. L. Phase relationship between hippocampal place units and the EEG theta rhythm. *Hippocampus*, 3:317–30, 1993.

- Pastalkova, E., Itskov, V., Amarasingham, A., and Buzsáki, G. Internally generated cell assembly sequences in the rat hippocampus. *Science*, 321:1322 – 1327, 2008.
- Polyn, S. M. and Kahana, M. J. Memory search and the neural representation of context. *Trends in Cognitive Sciences*, 12:24–30, 2008.
- Polyn, S. M., Natu, V. S., Cohen, J. D., and Norman, K. A. Category-specific cortical activity precedes retrieval during memory search. *Science*, 310:1963–1966, 2005.
- Polyn, S. M., Norman, K. A., and Kahana, M. J. A context maintenance and retrieval model of organizational processes in free recall. *Psychological Review*, 116:129–156, 2009a.
- Polyn, S. M., Norman, K. A., and Kahana, M. J. Task context and organization in free recall. *Neuropsychologia*, 47:2158–2163, 2009b.
- Quirk, G. J., Muller, R. U., Kubie, J. L., and Ranck, J. B., Jr. The positional firing properties of medial entorhinal neurons: Description and comparison with hippocampal place cells. *Journal of Neuroscience*, 12(5):1945–1963, 1992.
- Quiroga, R. Q., Nadasdy, Z., and Ben-Shaul, Y. Unsupervised spike detection and sorting with wavelets and superparamagnetic clustering. *Neural Computation*, 16:1661–1687, 2004.
- Ravassard, P., Kees, A., Willers, B., Ho, D., Aharoni, D., Cushman, J., Aghajan, Z. M., and Mehta, M. R. Multisensory control of hippocampal spatiotemporal selectivity. *Science*, 340(6138):1342–1346, 2013.
- Rutishauser, U., Ross, I., Mamelak, A., and Schuman, E. Human memory strength is predicted by theta-frequency phase-locking of single neurons. *Nature*, 464(7290):903–907, 2010.
- Sainsbury, R. S., Heynen, A., and Montoya, C. P. Behavioral correlates of hippocampal type 2 theta in the rat. *Physiology & behavior*, 39(4):513–519, 1987.
- Sargolini, F., Fyhn, M., Hafting, T., McNaughton, B., Witter, M., Moser, M., and Moser, E. Conjunctive Representation of Position, Direction, and Velocity in Entorhinal Cortex. *Science*, 312(5774):758–762, 2006.
- Scoville, W. B. and Milner, B. Loss of recent memory after bilateral hippocampal lesions. *Journal of Neurology, Neurosurgery, and Psychiatry*, 20:11–21, 1957.
- Sederberg, P. B., Kahana, M. J., Howard, M. W., Donner, E. J., and Madsen, J. R. Theta and gamma oscillations during encoding predict subsequent recall. *Journal of Neuroscience*, 23(34):10809–10814, 2003.
- Sederberg, P. B., Schulze-Bonhage, A., Madsen, J. R., Bromfield, E. B., McCarthy, D. C., Brandt, A., Tully, M. S., and Kahana, M. J. Hippocampal and neocortical gamma oscillations predict memory formation in humans. *Cerebral Cortex*, 17(5):1190–1196, 2007.
- Seidenbecher, T., Laxmi, T., Stork, O., and Pape, H. Amygdalar and hippocampal theta rhythm synchronization during fear memory retrieval. *Science*, 301(5634):846, 2003.
- Semba, K. and Komisaruk, B. Neural substrates of two different rhythmical vibrissal movements in the rat. *Neuroscience*, 12(3):761–774, 1984.
- Singer, A., Karlsson, M., Nathe, A., Carr, M., and Frank, L. Experience-dependent development of coordinated hippocampal spatial activity representing the similarity of related locations. *Journal of Neuroscience*, 30(35):11586, 2010.
- Skaggs, W. E., McNaughton, B. L., Wilson, M. A., and Barnes, C. A. Theta phase precession in hippocampal neuronal populations and the compression of temporal sequences. *Hippocampus*, 6:149–172, 1996.

- Solstad, T., Moser, E. I., and Einevoll, G. T. From grid cells to place cells: A mathematical model. *Hippocampus*, 16:1026–1031, 2006.
- Solstad, T., Boccara, C., Kropff, E., Moser, M., and Moser, E. Representation of Geometric Borders in the Entorhinal Cortex. *Science*, 322(5909):1865, 2008.
- Solway, A., Miller, J. F., and Kahana, M. J. PandaEPL: A library for programming spatial navigation experiments. *Behavior Research Methods*, 45(4):1293–1312, 2013.
- Solway, A., Geller, A. S., Sederberg, P. B., and Kahana, M. J. Pyparse: A semiautomated system for scoring spoken recall data. *Behavior Research Methods*, 42(1):141–147, 2010.
- Spiers, H. J., Hayman, R. M., Jovalekic, A., Marozzi, E., and Jeffery, K. J. Place field repetition and purely local remapping in a multicompartment environment. *Cerebral Cortex*, page bht198, 2013.
- Strange, B. A., Witter, M. P., Lein, E. S., and Moser, E. I. Functional organization of the hippocampal longitudinal axis. *Nature Reviews Neuroscience*, 15(10):655–669, 2014.
- Talairach, J. and Tournoux, P. *Co-planar stereotaxic atlas of the human brain*. Verlag, Stuttgart, 1988.
- Taube, J., Muller, R., and Ranck, J. Head-direction cells recorded from the postsubiculum in freely moving rats. I. Description and quantitative analysis. *Journal of Neuroscience*, 10(2):420–435, 1990.
- Terrazas, A., Krause, M., Lipa, P., Gothard, K., Barnes, C., and McNaughton, B. Self-motion and the hippocampal spatial metric. *Journal of Neuroscience*, 25(35):8085–8096, 2005.
- Tolman, E. C. Cognitive maps in rats and men. *Psychology Review*, 55:189–208, 1948.
- Tsao, A., Moser, M.-B., and Moser, E. I. Traces of experience in the lateral entorhinal cortex. *Current Biology*, 2013.
- Tulving, E. Episodic and semantic memory. In Tulving, E. and Donaldson, W., editors, *Organization of Memory*., pages 381–403. Academic Press, New York, 1972.
- Tulving, E. *Elements of Episodic Memory*. Oxford, New York, 1983.
- Vanderwolf, C. Hippocampal electrical activity and voluntary movement of the rat. *Electroencephalography and Clinical Neurophysiology*, 26:407–418, 1969.
- Watrous, A. J., Fried, I., and Ekstrom, A. D. Behavioral correlates of human hippocampal delta and theta oscillations during navigation. *Journal of Neurophysiology*, 105(4):1747–1755, 2011.
- Watrous, A. J., Lee, D. J., Izadi, A., Gurkoff, G. G., Shahlaie, K., and Ekstrom, A. D. A comparative study of human and rat hippocampal low-frequency oscillations during spatial navigation. *Hippocampus*, 2013.
- Wilson, M. A. and McNaughton, B. L. Dynamics of the hippocampal ensemble code for space. *Science*, 261:1055–8, 1993.
- Winson, J. Loss of hippocampal theta rhythms in spatial memory deficit in the rat. *Science*, 201:160–163, 1978.
- Wood, E. R., Dudchenko, P. A., and Eichenbaum, H. The global record of memory in hippocampal neuronal activity. *Nature*, 397:613–616, 1999.
- Wood, E. R., Dudchenko, P. A., Robitsek, R. J., and Eichenbaum, H. Hippocampal neurons encode information about different types of memory episodes occurring in the same location. *Neuron*, 27:623–633, 2000.

- Young, B. J., Fox, G. D., and Eichenbaum, H. Correlates of hippocampal complex-spike cell activity in rats performing a nonspatial radial maze task. *The Journal of neuroscience*, 14(11):6553–6563, 1994.
- Yushkevich, P. A., Pluta, J. B., Wang, H., Xie, L., Ding, S.-L., Gertje, E. C., Mancuso, L., Kliot, D., Das, S. R., and Wolk, D. A. Automated volumetry and regional thickness analysis of hippocampal subfields and medial temporal cortical structures in mild cognitive impairment. *Human brain mapping*, 36(1):258–287, 2015.
- Zhang, K., Ginzburg, I., McNaughton, B. L., and Sejnowski, T. J. Interpreting neuronal population activity by reconstruction: unified framework with application to hippocampal place cells. *Journal of neurophysiology*, 79(2):1017–1044, 1998.
- Zhang, S.-J., Ye, J., Miao, C., Tsao, A., Cerniauskas, I., Ledergerber, D., Moser, M.-B., and Moser, E. I. Optogenetic dissection of entorhinal-hippocampal functional connectivity. *Science*, 340(6128), 2013.

